Title
The Cell Transmission Model. Part I: A Simple Dynamic Representation Of Highway Traffic

Author
Daganzo, Carlos

Publication Date
1992

CALIFORNIA PATH PROGRAM
INSTITUTE OF TRANSPORTATION STUDIES
UNIVERSITY OF CALIFORNIA, BERKELEY

The Cell Transmission Model. Part I: A Simple Dynamic Representation of Highway Traffic

Carlos F. Daganzo

UCB-ITS-PRR-93-7

This work was performed as part of the California PATH Program of the University of California, in cooperation with the State of California Business, Transportation, and Housing Agency, Department of Transportation; and the United States Department of Transportation, Federal Highway Administration.

JULY 1993

ISSN 10551425

THE CELL TRANSMISSION MODEL. PART I: A SIMPLE DYNAMIC REPRESENTATION OF HIGHWAY TRAFFIC*

by

CARLOS F. DAGANZO

Department of Civil Engineering and
Institute of Transportation Studies
University of California, Berkeley CA 94720

Abstract

This paper presents a simple representation of traffic on a highway with a single entrance and exit. The representation can be used to predict traffic's evolution over time and space, including transient phenomena such as the building, propagation and dissipation of queues. The easy-to-solve difference equations used to predict traffic's evolution are shown to be the discrete analog of the differential equations arising from a special case of the hydrodynamic model of traffic flow. The proposed method automatically generates appropriate changes in density at locations where the hydrodynamic theory would call for a shockwave; i.e. a jump in density such as those typically seen at the end of every queue. The complex side calculations required by classical methods to keep track of shockwaves are thus eliminated. The paper also shows how the equations can mimic the real-life development of stop-and-go traffic within moving queues. The model predicts that the oscillation pattern is independent of the initial impulse from downstream (as one would expect), and that oscillations should not increase delay unless they result in car stalls or other incidents.

The results in this paper can be used for simple traffic engineering analyses. Most importantly, they are a fundamental building block for traffic prediction over networks. The ability to make such predictions can lead to better strategies for ramp metering and incident detection. A sequel to this paper will examine highway networks. The representation's simplicity should make it possible to keep track of each vehicle's final destination throughout a simulation, even for complex networks. This capability should help improve traffic control packages and dynamic traffic assignment methods.

* Research supported by PATH MOU 90, Institute of Transportation Studies, Berkeley, CA.

CONTENTS

LIST OF TABLES

updated with every tick of a clock.

To this end the road is divided into homogeneous sections (cells), numbered consecutively starting with the upstream end of the road, from i = 1 to I. The lengths of the sections are not chosen arbitrarily; they are set equal to the distances traveled in light traffic by a typical vehicle in one clock tick. Under light traffic then, all the vehicles in a cell can be assumed to advance to the next with each tick; it is unnecessary to know where within the cell they are located. Thus, the system's evolution obeys:

$$n_{i+1}(t+1) = n_i(t),$$

where ni(t) is the number of vehicles in cell i at time t. We will assume that the above recursion holds for all flows, unless traffic is slowed down by queueing from a downstream bottleneck. This seems reasonable because, for crowded conditions as might arise during the rush hour, most of the delays can be attributed to queueing at bottlenecks where flow temporarily exceeds capacity; rather than to any dependence between flow and speed. (It has been empirically observed that the space-mean speed of freeway traffic remains relatively constant, independent of flow, unless flow is close to capacity.)

To incorporate queueing we introduce two constants: $N_i(t)$, the maximum number of vehicles that can be present in cell i at time t, and $Q_i(t)$, the maximum number of vehicles that can flow into cell i when the clock advances from t to t+1 (time interval t). The first constant is the product of the cell's length and its "jam

density", and the second one is its "maximum flow (or capacity)". We allow these constants to vary with time to be able to model transient traffic incidents. The number of vehicles that can flow from cell i-l to cell i when the clock advances from t to t+1 (the flow into "i" for the time interval after "t"), yi(t) , is assumed to be the smallest of three quantities:

$n_{i-1}(t)$, the number of vehicles in cell i-l at time t,

$Q_i(t)$, the capacity flow into i for time interval t, and

$N_i(t)-n_i(t)$, the amount of empty space in cell i at time t.

(This last quantity ensures that the vehicular density on every section of the road remains below jam density.) Our proposed simulation, called the "cell-transmission model", will be based on a recursion where the cell occupancy at time t+1 equals its occupancy at time t, plus the inflow and minus the outflow; i.e.:

$$n_i(t+1) = n_i(t) + y_i(t) - y_{i+1}(t) \qquad (1a)$$

where the flows are related to the current conditions at time t as indicated above:

$$Yi(t) = \min\{ n_{i-1}(t) , Q_i(t) , N_i(t)-n_i(t) \}. \qquad (1b)$$

The simulation would step through time, updating the cell occupancies (for all i) with each tick of the clock.

Boundary conditions can be specified by means of input and output cells. The output cell, a sink for all exiting traffic, should have infinite size ($N_{I+1} = \infty$) and a suitable, possibly time-varying, capacity. Input flows can be modeled by a cell pair. A "source" cell numbered "00" with an infinite number of vehicles ($n_{00}(0) = \infty$) that discharges into an empty "gate" cell "0" of infinite size, $NO(t) = \infty$. The inflow capacity $Q_0(t)$ of the gate cell is set equal to the desired link input flow for time interval t+1. The gate cell then acts as a metering device that releases traffic at the desired rate while holding (as a parking lot would) any flow that is unable to enter the link.

Note that the result of the simulation is independent of the order in which the cells are considered at each step. This important property of the cell-transmission model will permit the analysis of complex networks, e.g. with loops. The property arises because we are specifying that the number of vehicles that enter a cell is unrelated to the number of vehicles that will leave it; thus, only current conditions influence the inflow to a cell. Although the first two restrictions ($y_i(t) \le n_{i-1}(t)$ and $y_i(t) \le Q_i(t)$) are reasonable in this regard, one may argue that if a cell is rapidly being emptied then the third (occupancy) restriction $y_i(t) \le N_i(t) - n_i(t)$ may be overly conservative. The counterargument is that empty slots for cars can only travel backwards at a finite speed (the wave propagation speed) unlikely to be greater than the free flow speed. Therefore the effects of

the outflow should only be noticed upstream after some time. Because this lag is one tick of the clock for our model, this is akin to assuming that density waves propagate backwards at the free flow speed. Sections 3 and 4 demonstrate that our simulation indeed behaves as a hydrodynamic model of traffic flow with this property.

3. EQUIVALENCE TO A HYDRODYNAMIC MODEL

We now consider a homogeneous highway and show that Eqs.(1) are a discrete approximation to the Lighthill, Whitham, Richards hydrodynamic model with a density-flow (k-q) relationship in the shape of an isosceles trapezoid, as in Fig. 1. This relationship can be expressed as:

$$q = \min\{ vk , q_{max} , v(k_j-k) \} , \qquad \text{for } 0 \le k \le k_j, \qquad (2)$$

where v is the free-flow speed (and the speed of all backward moving waves), kj is the jam density, and qmax $\le k_j v/2$ is the maximum flow.

If Eq.(2) is replaced into the flow conservation equation:

$$\delta q(x,t)/\delta x = -\delta k(x,t)/\delta t$$

we obtain the differential equation that would define the evolution of the system under the hydrodynamic model:

$$\delta \min\{ vk(x,t) , qmax , v(k_j - k(x,t)) \}/\delta x = -\delta k(x,t)/\delta t. \quad (3)$$

We now show that Eq.(3) is equivalent to our simulation. Note that for our homogeneous highway the cell characteristics would be independent of i and t: $N_i(t) = N$ and $Q_i(t) = Q$. To demonstrate the equivalence of the discrete and continuous approaches we now define the tick of the clock to be equal to dt and choose the unit of distance such that vdt = 1. Then the cell length is 1, v is also 1, and the following equvalences hold: $x \equiv i$, $k_j \equiv N$, $qmax \equiv Q$, and $k(x,t) \equiv n_i(t)$. With these conventions, the variable in braces in Eq.(3) is equivalent to:

$$\min\{ n_i(t), Q , N - n_i(t) \},$$

which coincides with the definition of $y_{i+1}(t)$ of Eqs.(1b), except for the subindex of n in the last term, which should have been i+1 instead of i. This, however, is immaterial unless the density is discontinuous. Because the hydrodynamic differential equations are only satisfied when the density is continuous with x (discontinuities —— shocks —— are treated outside of the differential equations with the hydrodynamic model) we can state that the variable in braces is equivalent to $y_{i+1}(t)$, and as a result the left hand side of Eq.(3) is:

$$y_{i+1}(t) - y_i(t) .$$

The right side of Eq(3), of course, is:

$$-[n_i(t+1) - n_i(t)]$$

and the equality of these two quantities justifies the simulation recursion, Eq.(1a).

To be sure, there are other forms of Eq.(1b) that would also be consistent with Eq.(3). For example, the flow into cell i, $y_i(t)$ could have been specified only as a function of the occupancy of the sending cell, i-l, so that Eq.(1b) would have been:

$$y_i(t) = \text{mint } n_{i-1}(t) \text{ , } Q_i(t) \text{ , } N_{i-1}(t)-n_{i-1}(t) \text{ }).$$

Alternatively, $y_i(t)$ could have been specified only as a function of the occupancy in the receiving cell. While these, and possibly other specifications are consistent with Eq.(3) for any slow varying density, their behavior in the face of discontinuities is not equivalent and may not be reasonable.

That consistency with Eq.(3) is no guarantee of reasonable behavior across discontinuities is clearly illustrated by the expression above. It should be clear from inspection that such an expression would predict zero flow downstream of any discontinuous drop in density from the jam density to any lower value. Thus, such a model would predict that vehicles queued at a traffic light would not advance even after the light turned green! (Unrealistic predictions also arise if flows are based only on the status of the receiving cell, as then a receiving cell would continue to attract

vehicles even after upstream occupancies have dropped to zero.)

Because discontinuities are common--arising spontaneously when low density traffic catches up with denser, slower downstream trafficfheir effect on model performance must be examined. We claim here that Eq.(1b) will replicate the behavior of the continuous model even across discontinuities. Thus, it should be possible to iterate Eqs.(1) and automatically track varying densities and the paths of any resulting shocks. This property, very useful for automatic computation, is discussed in the next two sections.

4. PROPAGATION OF DISTURBANCES AND CREATION OF SHOCKS

Here we compare the predictions of the hydrodynamic theory and our model, when the density along the road is known at an initial time (t = 0) and discontinuities may be created.

Consider a portion of road where the density varies within a narrow range in the direction of travel; i.e. k(x,O) changes with x, but remains either: (i) between 0 and k_A (in Figure 1), (ii) between k_A and kg, or (iii) between k_B and k_j. Then the hydrodynamic theory predicts that the same density profile will be preserved over time, except for a position shift; no shocks are created. That is, $k(x,t) = k(x-w_k t,0)$, where wk is the wave speed for the portion of the diagram corresponding to our initial densities. For our chosen time-distance units of measurement (with v = l)-the wave speed is 1 for case (i), 0 for case (ii), and —1 for case (iii). (This result arises because in the special case we

are considering the characteristics —— loci of constant density in time-space —— are parallel straight lines with slope w_k.)

It is not difficult to see that the cell-transmission model also satisfies k(x,t) = $k(x-w_kt,0)$: According to Eq.(1b) the number of vehicles transmitted from cell i-l to cell i is either n_{i-1}, Q_i, or N_i-n_i depending on whether k is in [O,kA], $[k_A,k_B]$ or $[k_B,k_j]$; and as a result, it should be clear from Eq.(1a) that $n_i(t+1)$ will be either ni-l(t), $n_i(t)$, or $n_{i+1}(t)$ depending on whether k is in [O,kA], $[k_A,k_B]$ or $[k_B,k_j]$. Thus the density profile (vehicle counts) move with the wave speed.

If the initial density profile is not entirely within a narrow range, the evolution is more complicated-discontinuities are created. We consider first situations when the density only increases in the direction of travel.

4.1 Increasing density

Let us assume that k(x,O) increases from a point slightly below k_A of Fig. 1 to a point above, and examine a range of x where the increase is roughly linear.

Without loss of generality, we assume that the units of measurement for time and space are chosen so that v = 1 (as before) and $\delta k(x,0)/\delta x = 1$. Further, we assume that vehicles are counted in units (e.g. pairs, halves, dozens...) such that the maximum flow is qmax = 50 units/time, and also assume that the origin of (spatial) coordinates is located where the initial density is 50 count units per unit distance. Thus, without any loss of generality we have reduced all the problems of interest to a unique

one for which the diagram of Fig.1 has only one free parameter kj (since qmax = 50, $k_A = 50$, and kg-kj $- k_A = k_j - 50$), and such that the initial density profile is k(x,O) = 50 + x. Furthermore, because neither kg nor kj affect the evolution of our density profile as long as the densities remain below kg, the free parameter doesn't need to be specified (we could select for example k_B = 100 and kj = 150).

Figure 2a depicts the map of characteristics for this problem and the shockwave resulting from the convergence of the characteristics. The shock path is defined by the line: x = t/2. On one side of the shock the density is defined by the horizontal characteristics and is k(x,t) = 50 + x; the flow is q(x,t) = 50. On the other side the density, defined by the slanted characteristics, is: 50 + x - t; the flow is q(x,t) = k(x,t). As the reader can easily verify, the curve in the figure is the only x(t) satisfying the vehicle conservation condition:

$$\delta x(t)/\delta t = [q_1(x,t)-q_2(x,t)]/[k_1(x,t)-k_2(x,t)], \quad (4)$$

where the subscripts "1" and "2" refer to the state on either side of the shock. (This condition ensures that vehicles don't disappear; i.e. those entering the shock on one side also leave it on the other side.)

Figure 2b depicts the density profile k(x,t) for different t. Note how the shock moves forward at speed 1/2, gradually increasing in size.

Figure 2c depicts the result of the cell transmission model,

Eqs.(1), when the initial conditions are as stipulated and the clock tick has been chosen to equal one time unit--this also implies that cells are one distance unit long. Note the similarity of Figs. 2c (viewed sideways) and 2a. The arrows in Fig. 2c follow the characteristics of constant density. The shock path, highlighted by circles between cells, alternates between 1 and 2 cells wide: as in Fig. 2a, it advances 1 cell (distance unit) for every 2 clock ticks. The rows of Fig. 2c are also consistent with the evolution pattern depicted in Fig. 2b.

The close agreement is not a result of the clock speed used. If a clock that was 10 times faster had been chosen, cells would have been 10 times shorter and the entries in the first row of Fig.2c would have been 10 times smaller. Because Q and N would also have been 10 times smaller, the result of the recursion would reveal the exact same pattern of Fig. 2c, except that the entries would have been 10 times smaller. Note in particular that the shock path would have remained 1 or 2 cells wide so that its actual spatial range would have been 10 times smaller than before. Thus, in agreement with the continuous hydrodynamic model, the spatial dimension of the shock could be made to vanish with infinitely fast clocks and negligible cell sizes.

A density profile k(x,O) that increases past k_B yields similar results. The same set of parameters for Fig. 1 (with $k_B = 100$ and $k_j = 150$) also suffices to describe this case exhaustively as long as the upstream density remains above k_A. As the reader can verify; the map of characteristics now is simply an upside down version of Fig 2a, with backward moving characteristics ahead of

stationary ones and a shockpath defined by x = -t/2. The numerical results of a simulation with first row cell contents increasing past "10 0" (... 98, 99, 100, 101, . ..) are also consistent with this pattern; as a whole they resemble an upside down version of Fig. 2c, including a backward moving shock that is 1 or 2 cells wide.

Suppose now that the density profile k(x,O) increases past k_A and then past kg. Then, the forward-moving shock generated when the density increases beyond k_A will eventually be met by the backward moving shock generated by the growth past kg. The shocks would coalesce into a (forward or backward) moving shock that would separate upstream traffic states with density in the interval $[0,k_A]$ from downstream traffic states with density in $[k_B,k_j]$. The speed of the coalesced shock would be governed by Eq.(4).

The numerical model replicates the behavior of the coalesced shock with a 1 or 2 cell interface that moves at the correct speed. That the interface must move at the speed given by Eq.(4) should be obvious since Eq.(4) is a direct result of vehicle conservation, and the numerical model conserves vehicles.[1] This fact is illustrated by the example in Sec. 5.

[1] To see that the interface only spans 1 or 2 cells, start with an initial set of occupancies such as (. . . . . n', n', n_0, n", n", . ..) where n' would correspond to a density below k_A, n" to a density above kg, and n_0 would be in the interval [n',n"]. Then, it suffices to check that at the next iteration there would be at most one cell with an occupancy different from n' and n", and that that cell could only be the cell previously containing n_0, or one of its neighbors. Care must be exercised in checking this property, because the flows between cells depend on the magnitude of n_0 relative to n', Q, N-Q, n" and N.

4.2 Decreasing density

With the flexibility to choose the units of measurement for counts, time and distance as described in Sec. 4.1, the diagram of Fig. 1 with $q_{max} = 50$, $k_A = 50$, kg = 100, and $k_j = 150$ still suffices to describe exhaustively the evolution of any density profile decreasing smoothly past either k_A or kg. The origin of spatial coordinates is chosen so that k(0,0) = 50 if the initial density profile decreases past k_A, and k(0,0) = 100 if it decreases past kg.

With these conventions, the maps of characteristics for both cases are as depicted in Fig. 3a. Because the characteristics diverge no shocks are formed; instead, constant-density, wedge-shaped regions appear in the time-space continuum. As shown in the figure, for a density decreasing past k_A the densities predicted by the hydrodynamic theory are:

$$\begin{aligned} k(x,t) &= k(x,0) \quad , \quad \text{if } x < 0 \\ &= k_A \quad , \quad \text{if } 0 \leq x \leq t \\ &= k(x-t,0) \quad , \quad \text{if } x > t. \end{aligned}$$

For a density decreasing past kg, the densities are:

$$\begin{aligned} k(x,t) &= k(x+t,0) \quad , \quad \text{if } x < -t. \\ &= k_B \quad , \quad \text{if } -t \leq x \leq 0 \\ &= k(x,0) \quad , \quad \text{if } x > 0. \end{aligned}$$

The figure also displays the density profile predicted by the hydrodynamic theory at $t = 0$ and 1 for both cases. In the first case densities below k_A are propagated forward at speed 1, and higher densities remain stationary; an expanding road section with density k_A separates the high and low densities. In the second case the low density section remains stationary and the high density section is propagated backward at speed -1.

Figure 3 also displays the results of the cell-transmission model, using as before a one time unit clock tick. The results closely replicate the hydrodynamic predictions. Note in particular the wedge-shaped regions of constant count and the direction of the characteristics.

We have thus established that if the density changes gradually over space, the cell transmission model is equivalent to the continuous hydrodynamic model. Discontinuities in this density (shocks) are also captured adequately by the cell-transmission model; they are represented by transition sections comparable with the lattice width and spanning 1 or 2 cells.

The next section presents an example involving the build-up and dissipation of a queue. Besides illustrating the phenomena discussed in Sec. 4, the example is also used as a venue to demonstrate the ease with which the numerical predictions can be automated.

5. IMPLEMENTATION AND EXAMPLE

As an illustration, we consider here a 1.25 mile homogeneous road with v = 50 MPH, k_j = 180 VPM and qmax = 3000 VPH. Initially traffic is flowing undisturbed at 80% of capacity: q = 2400 VPH. Then, a partial lane blockage lasting 2 min occurs 1/3 of the distance from the end of the road. The blockage effectively restricts flow to 20% of the maximum. Clearly, a queue is going to build and dissipate behind the restriction. We wish to predict the evolution of the traffic density on the road before, during and after the incident: both upstream and downstream of it.

If we choose a 6 second clock tick ($1/600^{th}$ of an hour), then the length of a cell must be 1/12 mile and there will be 15 cells. The cell constants are:

$$N = 15 \text{ and } Q = 5.$$

The incident is modeled by limiting the capacity of the 11^{th} cell to 1/5 of the maximum for the first two minutes; i.e.: $Q_{11}(t) = 1$ for $t \leq 20$. Initially, each cell contains $n_i(0) = (1/12)(q/v) = 4$ vehicles. The output cell flow constant is $Q_{21}(t) = 5$, and the maximum flow into the input "gate", QO(t) = 4.

With this information, it is a simple matter to iterate Eqs.(1). The result is displayed on Fig. 4. Although the figure was developed with a computer spreadsheet, the reader can easily verify manually that Eqs.(1) are satisfied by checking a

representative sampling of cells. The spreadsheet program, documented in the Appendix, can be easily copied by the interested reader; with minor modifications, it can be applied to other (single link) problems.

Figure 5 displays the vehicle trajectory-shockwave diagram that is obtained from the hydrodynamic theory. It has been plotted using the same scale as in Figure 4, so that direct comparisons can be made. The thin broken line starting at the origin represents a vehicle trajectory; the dark lines represent abrupt transitions between traffic states[2]. The capital letters identify the traffic states prevailing in each region of the time-space diagram. Note the close match of both the shockpaths and the densities in the different portions of both diagrams. The reader is encouraged to solve other problems with the spreadsheet provided in the Appendix, and to perform similar comparisons. As explained earlier, in examining the results one should expect discrepancies comparable to the size of a cell between the simulation and the continuous solution —— discrepancies that would be undetectable on a scale large compared with a tick of the clock.,

[2] The reader may recall that a graphical procedure involving the k-q diagram (shown in the corner) can be used to determine the slopes of the vehicle trajectories and the interfaces between different traffic states. Vehicle trajectories in a given state (e.g. "E") must be parallel to the line of the k-q diagram connecting the origin to the appropriate state (e.g. "E"). By virtue of Eq.(4), interfaces between two states must be parallel to the line in the k-q diagram connecting the two states in question.

6. THE CELL-TRANSMISSION MODEL: GENERAL CASE

Although the equation of state in Fig. 1 allows one to choose three basic engineering parameters (the free flow speed, the maximum flow and the jam density), the relationship forces the backward wave speed to match the free flow speed. This is somewhat unrealistic because in reality waves move several times more slowly than free flowing traffic, changing the manner in which vehicles approach the bottleneck and the location of queues. (With slow waves, queues persist for a longer time behind a temporary bottleneck and are dissipated further upstream.) On the other hand, the wave speed discrepancy can be shown not to change the time when approaching vehicles would pass a bottleneck and, hence, not to influence the resulting vehicle delay.

Here, thus, we examine an extension of the cell-transmission model that would approximate the hydrodynamic model for an equation of state that allows backward waves with speed $w \leq v$. Said equation of state, depicted in Fig. 6, is:

$$q = \min\{ vk , qmax , w(k_j - k) \}, \qquad \text{for } 0 \leq k \leq kj, \qquad (5)$$

where $w \leq v$ and $qmax \leq k_j/[1/v + 1/w]$.

The cell-transmission model intended to represent this relationship is identical in all respects to the one in Sec. 2, except-that Eq. (lb) is modified slightly and now is:

$$y_i(t) = \min\{ n_{i-1}(t) , Q_i(t) , (w/v)[N_i(t)-n_i(t)] \}. \qquad (6)$$

6.1. Equivalence to the hydrodynamic theory

For a homogeneous highway, the differential equation defining the evolution of the system under the hydrodynamic model, formerly given by Eq.(3), is now :

$$\delta \min\{ vk(x,t) , qmax , w(k_j-k(x,t)) \}/\delta x = -\delta k(x,t)/\delta t. \qquad (7)$$

In our discrete representation the cell characteristics should be independent of i and t, so that in Eq.(6), $N_i(t) = N$ and $Q_i(t) = Q$. As in Sec. 3 we define the tick of the clock to be equal to dt and choose the unit of distance such that vdt = 1. Therefore, the following equivalences hold: $x \equiv i$, $kj \equiv N$, $qmax \equiv Q$, $w = w/v$, and $k(x,t) \equiv n_i(t)$. With these conventions, the variable in braces in Eq.(7) is equivalent to:

$$\text{mint } q(t) , Q , (w/v)[(N-n_i(t)] \},$$

which except for the subindex of n in the first term is the definition of $y_i(t)$ according to Eqs.(6). For continuous density profiles the discrepancy in subscripts is immaterial; hence, the left hand side of Eq.(7) is equivalent to:

$$y_{i+1}(t) - y_i(t) .$$

The right side of Eq.(7), of course, is equivalent to:

$$-[n_i(t+1) - n_i(t)]$$

Clearly then, Eq. (7) and the finite difference recursion (la) must be equivalent when the density is continuous, since both simply state the equality of the above two quantities.

As before, the subindices chosen for Eq.(6) ensure that the recursion behaves properly in the presence of discontinuities. The following subsection explores this fact in more detail.

6.2 Behavior of difference equations with finite clock ticks

As happened for the basic cell-transmission model, finite difference equations (la) and (6) solve the continuous hydrodynamic model of Fig. 6 when an infinitesimally small clock tick is used. We now explore the model behavior with finite clock ticks and discontinuous densities. Sections 4 and 5 demonstrated that for finite clock ticks the difference between the continuous and discrete solutions to the basic model is minimal: the largest discrepancy between the two arises with the representation of shocks, which take no space in the continuous model but span either 1 or 2 cells in the discrete model. The generalized model, although equivalent to the continuous model in the limit, is not as well behaved for finite clock ticks.

To illustrate the issues, the current subsection describes the evolution of both a shock and an acceleration wave, as predicted by both the continuous and discrete equations. Then, the following

sub-section introduces a modification to Eq.(6) that improves the finite clock tick performance of the model.

In this subsection we will use the diagram of Fig. 6 with $v = 1$ and $k_A = 50$ (no loss of generality here), and will also assume when an illustration is needed that w = 0.25 (a reasonable value) and $kg = k_A$. As a result, qmax = 50 and $k_j = 250$.

Consider first a density profile, representing traffic running into the back of a stationary queue at position x = 15; i.e.:

$$k(x,0) = k \quad \text{if } x < 15$$
$$= k_j \quad \text{if } x \geq 15.$$

The discontinuity at x = 15 is a shockwave that will propagate backward. If k is greater than kg (e.g. k = 70), then the shock will propagate at speed -0.25 (see Fig. 6).

In a plot of cumulative vehicle count (recall that we may be counting vehicle pairs, dozens, etc) vs. distance, the shock will appear as a convex break in the slope of the curve. The position of this break is independent of the count label assigned to the vehicle at x = 0, and for this reason we will always assign label 0 to the vehicle immediately upstream of x = 0; then the cumulative count K(x,t), called from now on the "cumulative profile", is the integral over x of k(x,t). (Note that this scheme does not identify individual vehicles). For our example, the initial cumulative profile is:

$$K(x,0) = xk \qquad \text{if } x < 15$$
$$= 15k + (x-15)k_j, \qquad \text{if } x \geq 15.$$

Because the shock travels at speed 0.25 the break in slope is at $x = 15-0.25t$ for any $t > 0$. Hence, for any $t < 40$, the cumulative profile predicted by the hydrodynamic theory is:

$$K(x,t) = xk \qquad \text{if } x < 15-0.25t$$
$$= (15-wt)k + [x-(15-wt)]k_j, \qquad \text{if } x \geq 15-0.25t.$$

The cumulative profile can also be evaluated with the cell-transmission model. If the clock ticks once every time unit and cells are defined so that cell 1 extends from $x = 0$ to $x = 1$, then the cumulative profile at any (integer valued) x is simply the sum of the vehicle counts in cells 1 to x-l. For the case with k_j -250 and $k = 70$, the initial cell contents would then be: (..., 70, 70, 250, 250,...). Figure 7 displays the approximation to K(x,t) at various times; dashed lines show the exact result. Notice how as time passes the discrete approximation "softens" the shock, so that it spreads to a growing number of cells.

A similar spreading phenomenon occurs with acceleration waves (i.e. concave bends in the cumulative profiles). Figure 8 depicts the results when the initial density profile is:

$$k(x,0) = k_j, \qquad \text{if } x < 10$$
$$= 50, \qquad \text{if } x \geq 10,$$

as if a blockage at x = 10, causing a stationary queue, had been removed at t = 0.

We claim that the prediction errors caused by numerical spreading are minor because as seen in Figs. 7 and 8: (i) the maximum error in the count increases at a decreasing rate with the passage of time, (ii) the disturbances still travel at the appropriate speed, (iii) the vehicle counts and densities on either side of the shock (or wave) are not corrupted, and (iv) the accuracy of the count near a shock (or wave) can be controlled by modifying the clock tick —— as per dimensional arguments already seen.

6.3. A modification that eliminates spreading for certain shocks

We had seen at the end of Sec. 3 that Eq.(1b) was not the only mechanism for defining an inter-cell flow that was consistent with Eq.(3) of the hydrodynamic theory, and that other formulations might not behave properly in the face of discontinuities.

Here we suggest a simple modification to Eq.(6) that behaves properly in the face of discontinuities and yet eliminates spreading of shocks separating a downstream density greater than k_A from an upstream density lower than k_A. The modified expression is:

$$y_i(t) = \min\{ n_{i-1}(t) , Q_i(t) , \alpha[N_i(t)-n_i(t)] \}, \qquad (8a)$$

where

$$\alpha = 1 \quad , \quad \text{if} \quad n_{i-1}(t) \leq Q_i(t) \qquad (8b)$$

$$= w/v \quad , \quad \text{if} \quad n_{i-1}(t) > Q_i(t). \qquad (8c)$$

It is not difficult to see following the logic of Sec. 6.1 that the expression is still consistent with the hydrodynamic theory when the n_i vary slowly.

We claim that with this correction any errors in the cumulative count near a shock (wave) should disappear once upstream light traffic ($v = 1$, $k < k_A$) catches up with the spreading shock (wave), and that as a result any numerical errors should be short lived. We base this observation on the fact that the shock preceeding the light traffic is of the non-spreading type, and that it eventually must separate accurate upstream and downstream counts.

Perhaps, the above argument can be best understood if it is illustrated with an example. Consider the following initial density profile:

$$k(x,0) = k_j \quad \text{if } 8 \leq x \leq 11$$
$$= 25 \quad \text{otherwise.}$$

A diagram of k(x,t) for this problem, also displaying the acceleration waves and shocks predicted by the hydrodynamic theory, is provided in Fig. 9b. It can be seen from it that all the changes in density for this problem are discontinuous, and that as a result the cumulative profile K(x,t) at any t should be a piecewise linear function, as shown in Fig. 9c. The solid lines in Fig. 10 are graphs of the cumulative profile for t = 0, 8, 16, 24 and- 32 as predicted with Eqs.(1a) and (8); the dashed lines in the figure are the (piecewise linear) exact results. Although the

acceleration waves spread (as shown by the concave bends of the curves), the (convex) shocks remain sharp. The figure clearly illustrates how the spreading wave is gradually "eaten up" by the advancing shock, until at time 24 and thereafter the exact and approximate results essentially coincide.

7. INSTABILITY

So far we have argued that the cell-transmission model in one of its forms can easily produce results consistent with the hydrodynamic theory of traffic flow. This section takes an extra step; it shows that the cell-transmission model has the potential for capturing real-life instability phenomena, not included in the hydrodynamic theory.

Research on the stop-and-go phenomenon of congested freeway traffic dates back at least to Edie and Foote's (1961) and Edie's (1963) observations at the Lincoln and Holland Tunnels, and the George Washington Bridge in New York. Despite substantial efforts on the subject since then (witness for example the extensive car-following literature of the 1960's) a model of traffic instability that would account for the long periods of oscillation (approximately 1 minute long) observed in practice seems to have eluded researchers.

Newell (1963) had stated that an instability would arise if drivers catching up with denser/slower traffic ahead were to delay braking, perhaps in the hope that traffic would clear up before they had to slow down. This behavior would result in average

spacings shorter than usual when traffic was decelerating (as observed by Edie) and would cause an instability. Of course, a microscopic car-following model to mimic this behavior would be extremely difficult to build (and validate) because in making their decisions drivers consider the recent evolution of the traffic stream immediately ahead, and not just the current status of one vehicle. A macroscopic model, consistent with Edie's observation that spacings are shorter when platoons are compressing, may be a more sensible goal to pursue.

Perhaps because of these difficulties, current efforts (see for example Ferrari, 1991) typically avoid seeking a behavioral explanation for instability and tend to focus instead on its control, using on-line macroscopic traffic measurements. This section also examines instability at the macroscopic level. It shows that the cell-transmission model, with a very simple modification that makes it consistent with Edie's observations, can duplicate real-life instability features.

Here we postulate that drivers operate in one of two modes depicted by the two q-k diagrams of Fig.11a, depending on the traffic conditions prevailing in a "look-ahead" road section extending a fixed distance ahead of their current location. If the traffic density in this "look-ahead" section is greater than the traffic density in the vehicles' immediate neighborhood (assumed to be smaller than the "look-ahead" section), then we will assume that the vehicles would advance position as if they were regulated by the top curve of the figure. Otherwise they will

advance according to the lower curve[3].

The cell-transmission model can capture such conditions quite naturally. Without loss of generality we define the cell length to be the distance of "the immediate neighborhood", and examine a special case where the "look-ahead" distance is two cells. Then, only the occupancies of two neighboring cells need to be compared to determine any inter-cell flow. For the purposes of illustration the q-k curves are assumed to be of the special form depicted in Fig.11b, as then no additional parameters need to be introduced. For this special case, the cell-transmission model will capture the desired behavior if the variable a of Eq. (8a) is redefined as:

$$a = 1 \quad \text{if} \quad n_{i-1}(t) \leq n_i(t) \text{ or } Q_i(t) \qquad (9a)$$

$$= w/v \quad , \quad \text{otherwise.} \qquad (9b)$$

Although much experimental evidence would be needed to make a strong claim for realism, the results described below at least seem to be qualitatively consistent with real-life behavior.

7.1 Results

Here we describe the numerical results of a number of

[3] Other conditions for the on-off switching mechanism could have been postulated. For example we could have stipulated that drivers will advance more aggressively (according to the upper curve) if the traffic density in their neighborhood has been increasing in time. Alternatively, aggressive behavior could be stipulated when both conditions are met (or else either one of them). Fortunately the specific trigger is not important because, with backward moving waves (relative to a vehicle) as result from our model, if one of the conditions is met so are the others; all the models should be similar.

simulations that were done with the cell-transmission model, using Eqs. (8a) and (9). The tests involve a homogeneous finite section of highway with a large input flow and a restricted steady output. Because the output is constant, the (stable) hydrodynamic steady state solution is a spatially uniform density. (The value of said density is given by the point on the congested part of the q-k curve that has q equal to the output flow.) If the system is assumed to be in steady state at time t = 0, Eqs. (9) don't generate any instability; they produce the same result as Eqs.(6) and Eqs.(8), of course matching the hydrodynamic prediction.

We explore here the evolution of the system as predicted by Eqs. (9) when a single random disturbance to the exit flow is introduced at time t = 0 (i.e a slightly larger or smaller output flow for the first clock tick only). Experiments have been conducted for a number of examples, and these will be discussed here qualitatively. Numerical results will be given for one of the examples (for illustration only) corresponding to the following parameters of Fig.11b : q_{max} (Q_i) = 50, k_j (Ni) = 150, w/v = 0.5; and the following initial conditions : Q_{output} = 25 and ni = 100.

In all the cases tested, and independently of the magnitude of the initial impulse, a flow disturbance was generated that grew in duration and magnitude as it traveled backward. The disturbance is first noticed by a temporary increase in flow, which is then followed by a shorter but sharp reduction, finally terminating with a gradual return to normalcy. The disturbance does not generate any lasting effects; after its passage, vehicles are observed to go by any location at the time they would have passed without the

disturbance. However, affected vehicles are observed to pass... earlier! We are not sure whether this would also occur in reality, and unfortunately it seems difficult to design an experiment to verify it. In a way the answer to this question is moot because, with a constant output flow, every vehicle will pass the bottleneck at its appointed time. A small disturbance cannot cause any delay.[4]

Figure 12a contains plots of cumulative count vs. time at 4 locations separated by 3 cells. Notice how the disturbance grows as described, eventually including intervals with nearly zero flow. From the time at which the shock front (the crest of each cumulative count curve) passes the various locations we can infer the disturbance's speed. In the figure, as in the other cases tested, the disturbance traveled (roughly) with the wave speed w. This should not be surprising for a disturbance that is no longer growing: the disturbance must move with the speed of its decreasing density portion, which must be w since Eqs.(9) and (8) are equivalent when the density decreases.

We also performed experiments in which a steady random noise was added to the exit flow—the noise was identical to the described impulse at t = 0 but operating at all times. With such noise, regularly oscillating waves would invariably develop upstream from the exit, with a period of oscillation that was the same at all locations and a phase shift of speed w. Both the wave

[4] We are assuming here that there are no side effects due to instability. In reality, oscillations could cause incidents and car stalls which would cause occasional delays. This benefit—and not wholesale reductions in delay due to an increased capacity—should be the justification for controls to smooth traffic out.

growth pattern and the oscillation period were surprisingly reproducible, i.e.largely independent of the set of generating impulses, perhaps providing an explanation for the regularity of stop-and-go traffic waves. Figure 12b illustrates these comments; the figure represents a situation identical in all respects to 12a, except that the single impulse has been replaced by steady noise. This figure can be compared with the flow-wave results of Edie and Foote (1959), given in Fig. 13. Note that a certain regularity was also observed in these experiments and that, as in Fig. 12, the disturbances also grew with the distance from the tunnel's exit.

For the same combination of parameters, Fig. 14 depicts the oscillations recorded in the q-k plane. Each point in the figure corresponds to a combination of $y_i(t)$ and the average of the occupancies in the sending and receiving cells during the two time intervals immediately preceeding and following clock tick i:

$$(1/4)[n_{i-1}(t)+n_i(t)+n_{i-1}(t+1)+n_i(t+1)].$$

The pattern of the figure, insensitive to the impulse set, is also observed at other locations although, obviously, there will be a scaling discrepancy wherever the disturbance is not fully grown. Different patterns, also insensitve to the impulse set and the specific location, are obtained for other wave speeds and initial densities.

The number of ticks for one oscillation was found to decline with w and to depend on the metering rate; the number was close to $8/(w/v)$ for $q \approx q_{max}/2$. Thus, a period of a few minutes as

observed in Fig. 13, would arise with w/v = 6 and a clock tick of about 5 seconds — the "look-ahead" section would then be a few hundred feet long.

Our findings seem to be consistent with the observations of Treiterer and Myers (1974) who documented the growth of one disturbance. Interesting to note is the similarity of Fig. 14 and Fig. 4 of this reference (reproduced here as Fig. 15a); the similarity should be qualified, however, because Treiterer and Myers' figure depicts the q-k oscillations seen by a moving observer and Fig. 13 does not. Other comparisons can also be made. From the trajectories in Treiterer and Myers' Fig. 2 (reproduced here as Fig. 15b) the following parameters can be estimated: v = 54 MPH, q_{max} = 1850 VPH, and k_j = 240 VPM. For a diagram such as the lower one of Fig. 11b this corresponds to a wave speed of about 9 MPH (consistent with the observed speed of the disturbance). We used a cell-transmission model with a 1.0 sec. clock tick and 0.015 mi. cell length, which ensures that v = 1 cell per tick = 54 MPH. With these basic features, the parameters of the cell-transmission model are: N = 3.6, Q = .51 and w/v = 1/6. The original state observed in the figure ($k \approx 80$ VPM > k_{op}) corresponds to n = 1.2. In rough agreement with the trajectory pattern of Fig. 13, the numerical results revealed a disturbance that grew in spatial dimension by about 60 meters per minute, traveling at about 7 MPH during this transitional phase.

The above comparisons are not meant to establish the validity of the model in Fig. 11b; only that it may have the potential for reproducing real-life phenomena. A very large empirical effort

would be needed to pinpoint more precisely a "correct" model. After all, typical instability features such as a disturbance's growth rate and its final equilibrium size may depend on local conditions, perhaps even changing across facilities just as k_j, q_{max}, w and v do. Besides changing the clock tick (and cell size), reducing the slope of the upper curve of Fig. 11b and increasing the number of cells for the "look-ahead" section might also capture these variabilities. The clock tick should be adjusted to match observed oscillation periods and the upper slope to match the disturbance's growth pattern. (We have found from our experiments that with a shallower upper branch for the diagram in Fig.11b the system becomes more stable, and when disturbances grow they grow at a slower rate.) We have not explored the effect of longer "look-ahead" sections. Another generalization might involve a model where the transition flows (8a) themselves include random noise.

8. CONCLUSION

Although the results in Secs. 6 and 7 have been developed for the specific form of the q-k relationship depicted in Fig. 6, the form is rather general. It offers 4 degrees of freedom: the free flow speed, the maximum flow, the jam density and the wave speed. As pointed by Newell (1991), these are the most important determinants of traffic evolution; and even if a more general model was available, it is unlikely that in any practical application an engineer would have reliable data beyond these parameters. Arguably, thus, a model with so much flexibility should be accurate

enough for modeling complex networks. This section presents some ideas that should be useful for network modeling; it first discusses the efficient calculation of various measures of performance, and then the possibility of using large clock ticks.

8.1 Measures of performance

From the information in a diagram such as Fig. 2 it is possible to recover any information. For network simulations, however, we would like to avoid storing in memory all the cell occupancy information for the duration of the simulation. The following shows how three important measures of performance can be calculated without using any extra memory.

The total number of vehicle-hours. The total number of vehicle-hours spent in any cell is simply the addition of $n_i(t)$ across t. The addition across cells yields the total time in the system for all users.

The total delay. The total number of vehicles to have left cell i is the addition of $y_{i+1}(t)$ across t. If the number of vehicles to have left cell i is equal to the number to have entered, then the added quantity represents the number of vehicles to have flowed through cell i. This is likely to happen for long periods of observation. Because in our measurement units $v = 1$, this number is also the total time that vehicles would have spent in cell i had they been able to travel freely. Therefore, the "delay" in cell i is:

$$\Sigma_t \{ n_i(t) - y_i(t) \}.$$

As with total time, the addition across cells yields the total delay.

The virtual time. We also define the "virtual time" in cell j as the time that would be spent in the cell by a vehicle about to enter it, if the current cell discharge rate was maintained. This virtual time may be useful in the planned sequel, for dynamic route guidance.[5] The ratio $n_i(t)/y_{i+1}(t)$ is the "virtual time"; it represents the number of ticks of the clock needed to empty cell i at the current emptying rate. Note that Eq.(1b) guarantees that the numerator is no smaller than the denominator. Logically then, the virtual time is never smaller than 1. (We define the ratio to be 1 if both the numerator and denominator are zero).

8.2 Large clock ticks

The method is very robust and returns accurate results, even for long clock intervals and large cell sizes. Errors in timing are comparable to the clock interval and errors in location are comparable to the cell size. Thus, in any practical application one should choose the longest clock step consistent with one's objectives.

To illustrate this property, the example of Figs. 4 and 5 can be repeated with a clock interval 5 times larger (30 sec.). In that case there will only be 3 cells (two upstream and one downstream of

[5] Recent research has cast some doubt on the usefulness of this concept.

the incident) and we will not be able to pinpoint precisely the location of vehicles within the highway. We are interested in assessing the impact of this lack of information on the flows that would be predicted at the entrance and exit to the highway, and on the total user time spent in the system.

Because less than 20 clock ticks are necessary, the calculations can be easily done manually. The cell constants are $Q = 25$ and $N = 75$; initially there are 20 vehicles in each cell. The reader can verify that the result in Table I is obtained. From the table we can verify that: (i) the flows through the restriction and at the exit vary in the same manner and return to normal at the same time as with the more detailed partition; (ii) as with the more detailed partition, the disturbance is not felt at the generator cell and hence the input flow into the road is steady in both cases; (iii) the total time in the system is the same in both cases — an obvious consequence of (i) and (ii). As in Newell's method, it seems that the system evolution (including flows and total time) can be predicted without tracking precisely the location of the vehicles within the highway.

REFERENCES

EDIE, L.C. (1963) "Traffic stream measurements and definitions", Proc. 2nd Int. Symp on the Theory of Traffic Flow: London 1963, J. Almond (editor), pp 139-154. Published by OECD, Paris, France, 1965.

EDIE, L.C. and FOOTE, R.S., (1959) "Experiments on single-lane flow in tunnels", Proc. 1st Int. Symp on the Theory of Traffic Flow: Warren MI 1959, R. Herman (editor), pp. 175-192. Published as Theory of Traffic Flow, Elsevier Publ. Co., New York, N.Y, 1961.

FERRARI, P. (1991) "The control of motorway reliability", Trans Res. 25A (6), 419-427.

HURDLE, V.F. (1991) "A theory of traffic flow for congested conditions on urban arterial streets I: 4 illustrative examples"(in press).

LIGHTHILL, M.J. and J.B. WHITHAM (1955) "On kinematic waves. I Flow movement in long rivers. II A theory of traffic flow on long crowded roads" Proc. Royal Soc. A 229, 281-345.

LUKE, J.C. (1972) "Mathematical models for landform evolution", J. Geophysical Research 77, 2460-2464.

NEWELL, G.F. (1963) "Instability in dense highway traffic: a review" Proc. 2nd Int. Symp on the Theory of Traffic Flow: London 1963, J. Almond (editor), pp 73-83. Published by OECD, Paris, France, 1965.

NEWELL, G.F. (1991) "A simplified theory of kinematic waves: I general theory; II queuing at freeway bottlenecks; III the 'traffic assignment problem' for freeways", Institute of Transportation Studies Research Report UCB-ITS-RR-91-12, University of California, Berkeley, 1991. (submitted for publication)

RICHARDS, P.I. (1956) "Shockwaves on the highway" Opns. Res. 4, 42-51.

SHEFFI, Y. (1985) Urban Transportation Networks: Equilibrium Analysis with Mathematical Programming Methods, Prentice-Hall, Englewood Cliffs, N.J.

TREITERER, J. and J.A. MYERS (1974) "The hysteresis phenomenon in traffic flow", Proc. 6th Int. Symp. Trans. and Traffic Theory, D.J. Buckley (editor), pp 13-38. A.H. & A.W. Reed, Sydney, Australia.

VAUGHAN, R. AND V.F. HURDLE (1991) "A theory of traffic flow for congested conditions on urban arterial streets I: Theoretical developments" (in press).

VAUGHAN, R., V.F. HURDLE AND E. HAUER (1984) "A traffic flow model with time-dependent O-D patterns" Proc. 9th Int. Symp. Trans. and Traffic Theory, J. Vollmuller and R. Hamerslag eds. Utretch, VNU Science Press pp.155-178.

TABLE I

Result of a simulation with a 30 sec. clock.
(Numbers indicate the number of vehicles in each cell).

Clock ticks (30 sec.)	Cell number			
	0	1	2	3
1	20	20	20	20
2	20	20	35	5
3	20	20	50	5
4	20	20	65	5
5	20	30	70	5
6	20	45	50	25
7	20	40	50	25
8	20	35	50	25
9	20	30	50	25
10	20	25	50	25
11	20	20	50	25
12	20	20	45	25
13	20	20	40	25
14	20	20	35	25
15	20	20	30	25
16	20	20	25	25
17	20	20	20	25
18	20	20	20	20

APPENDIX

APPENDIX

Spreadsheet documentation

Table II displays the first few rows of the spreadsheet used to simulate our link. The remaining rows up to row 115 are similar. All the entries of the spreadsheet are data, except for range E17..T115. In particular, note rows 12 and 13, which contain the cell constants. The maximum flow for highway section 11 is not provided because that is the section with the time varying capacity. The pertaining information is instead provided on column "V". By changing the entries to this column, one can model incidents of different duration and severity. Row 16 represents the initial conditions.

The formula for cell E17, the equivalent of Eqs.(1), is:

```
+E16-@MIN(E16,F$12,F$11-F14)+@MIN(D16,E$12,E$13-E16).
```

It is copied to range E17..T115, except for columns "O" and "P", which cannot address spreadshhet cell "P$12". This argument should be replaced by the capacity given in column V for the prior clock tick: "V16" is used for row 17. Calculation of the spreadsheet will then produce the data displayed in the table (and in Fig. 2).

TABLE II
Structure of the spreadsheet program

	C	D	E	F	G	H	I	J	K	L	M	N	O	P	Q	R	S	T	U	V	W
2																					
3	This spreadsheet simulates a link with 15 cells of capacity Ni																				
4	fed continuously from an upstrean generator. The density																				
5	diagram, with shockwaves can be seen at a glance.																				
6																					
7	Generator cells																		Output		
8	Source	Gate					Cell #												cell		
9													*								
10		00	0	1	2	3	4	5	6	7	8	9	10	11	12	13	14	15	16		
11																					
12	Qi=N/A	4	5	5	5	5	5	5	5	5	5	5	N/A	5	5		5	5	5	Q11(t)	
13	Ni=N/A	99	15	15	15	15	15	15	15	15	15	15	15	15	15	15	15	15	99		
14																					
15	Time																				
16	1	99	4	4	4	4	4	4	4	4	4	4	4	4	4	4	4	4	1		
17	2	99	4	4	4	4	4	4	4	4	4	4	7	1	4	4	4	4	1		
18	3	99	4	4	4	4	4	4	4	4	4	4	10	1	1	4	4	4	1		
19	4	99	4	4	4	4	4	4	4	4	4	4	13	1	1	1	4	4	1		
20	5	99	4	4	4	4	4	4	4	4	4	6	14	1	1	1	1	4	1		
21	6	99	4	4	4	4	4	4	4	4	4	9	14	1	1	1	1	1	1		
22	7	99	4	4	4	4	4	4	4	4	4	12	14	1	1	1	1	1	1		
23	8	99	4	4	4	4	4	4	4	4	5	14	14	1	1	1	1	1	1		
24	9	99	4	4	4	4	4	4	4	4	8	14	14	1	1	1	1	1	1		
25	10	99	4	4	4	4	4	4	4	4	11	14	14	1	1	1	1	1	1		
26	11	99	4	4	4	4	4	4	4	4	14	14	14	1	1	1	1	1	1		
27	12	99	4	4	4	4	4	4	4	7	14	14	14	1	1	1	1	1	1		
28	13	99	4	4	4	4	4	4	4	10	14	14	14	1	1	1	1	1	1		
29	14	99	4	4	4	4	4	4	4	13	14	14	14	1	1	1	1	1	1		
30	15	99	4	4	4	4	4	4	6	14	14	14	14	1	1	1	1	1	1		
31	16	99	4	4	4	4	4	4	9	14	14	14	14	1	1	1	1	1	1		
32	17	99	4	4	4	4	4	4	12	14	14	14	14	1	1	1	1	1	1		
33	18	99	4	4	4	4	4	5	14	14	14	14	14	1	1	1	1	1	1		
34	19	99	4	4	4	4	4	8	14	14	14	14	14	1	1	1	1	1	1		
35	20	99	4	4	4	4	4	11	14	14	14	14	14	1	1	1	1	1	1		
36	21	99	4	4	4	4	4	14	14	14	14	14	14	1	1	1	1	1	5		
37	22	99	4	4	4	4	7	14	14	14	14	14	10	5	1	1	1	1	5		
38	23	99	4	4	4	4	10	14	14	14	14	10	10	5	5	1	1	1	5		
39	24	99	4	4	4	4	13	14	14	14	10	10	10	5	5	5	1	1	5		
40	25	99	4	4	4	6	14	14	14	10	10	10	10	5	5	5	5	1	5		
41	26	99	4	4	4	9	14	14	10	10	10	10	10	5	5	5	5	5	5		
42	27	99	4	4	4	12	14	10	10	10	10	10	10	5	5	5	5	5	5		
43	28	99	4	4	5	14	10	10	10	10	10	10	10	5	5	5	5	5	5		
44	29	99	4	4	8	10	10	10	10	10	10	10	10	5	5	5	5	5	5		
45	30	99	4	4	7	10	10	10	10	10	10	10	10	5	5	5	5	5	5		
46	31	99	4	4	6	10	10	10	10	10	10	10	10	5	5	5	5	5	5		
47	32	99	4	4	5	10	10	10	10	10	10	10	10	5	5	5	5	5	5		

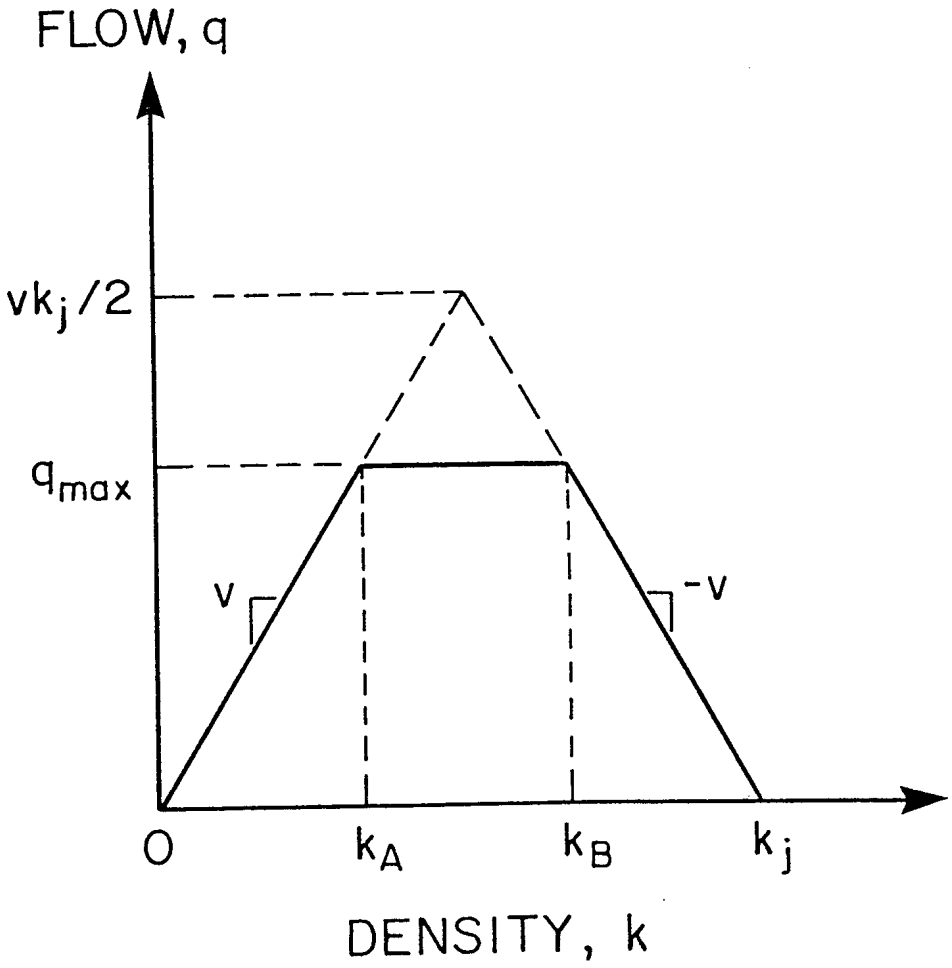

Figure 1. Flow-density relationship for the basic cell-transmission model.

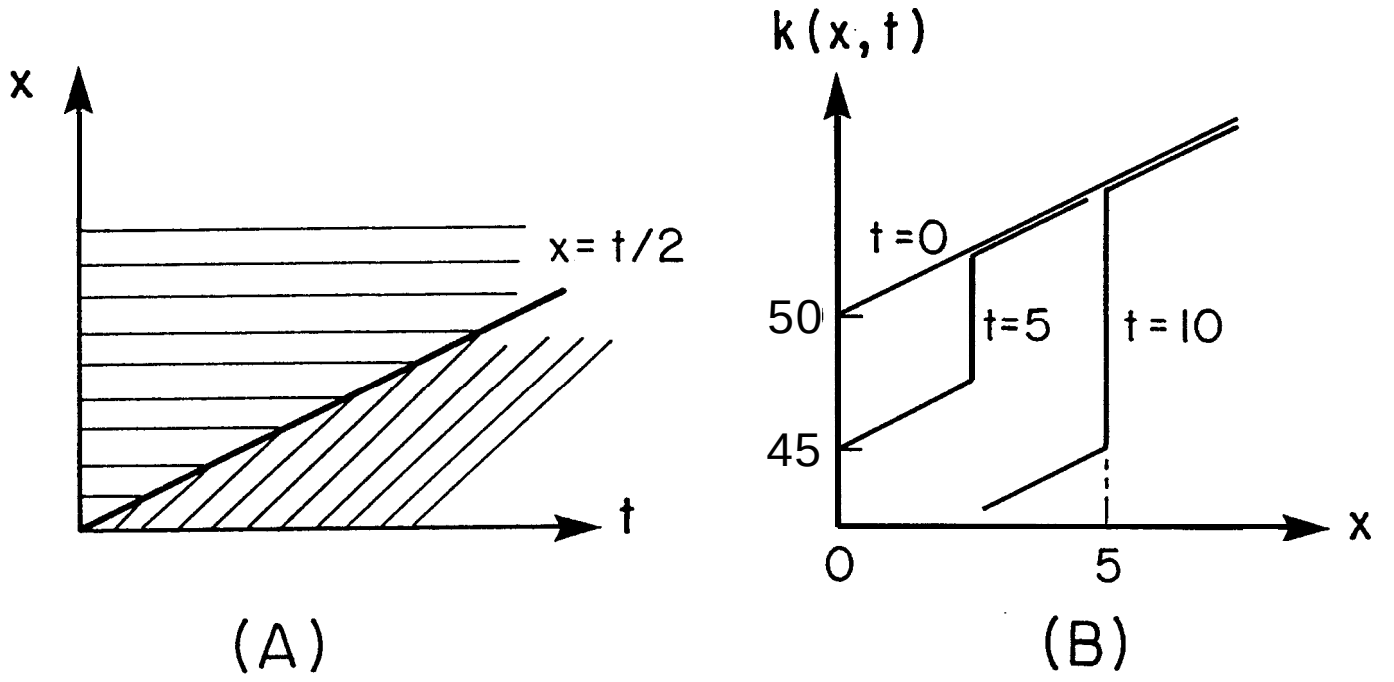

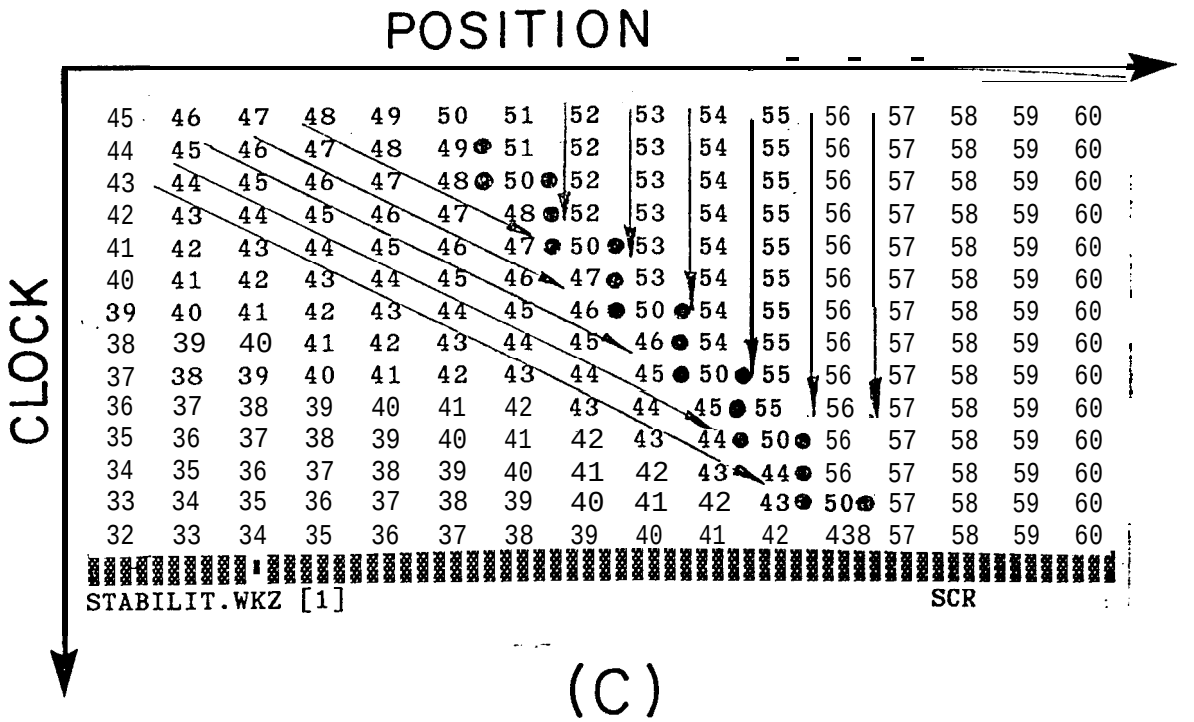

Figure 2. Traffic evolution with an increasing density. (a) Map of characteristics. (b) Density profile. (c) Numerical result.

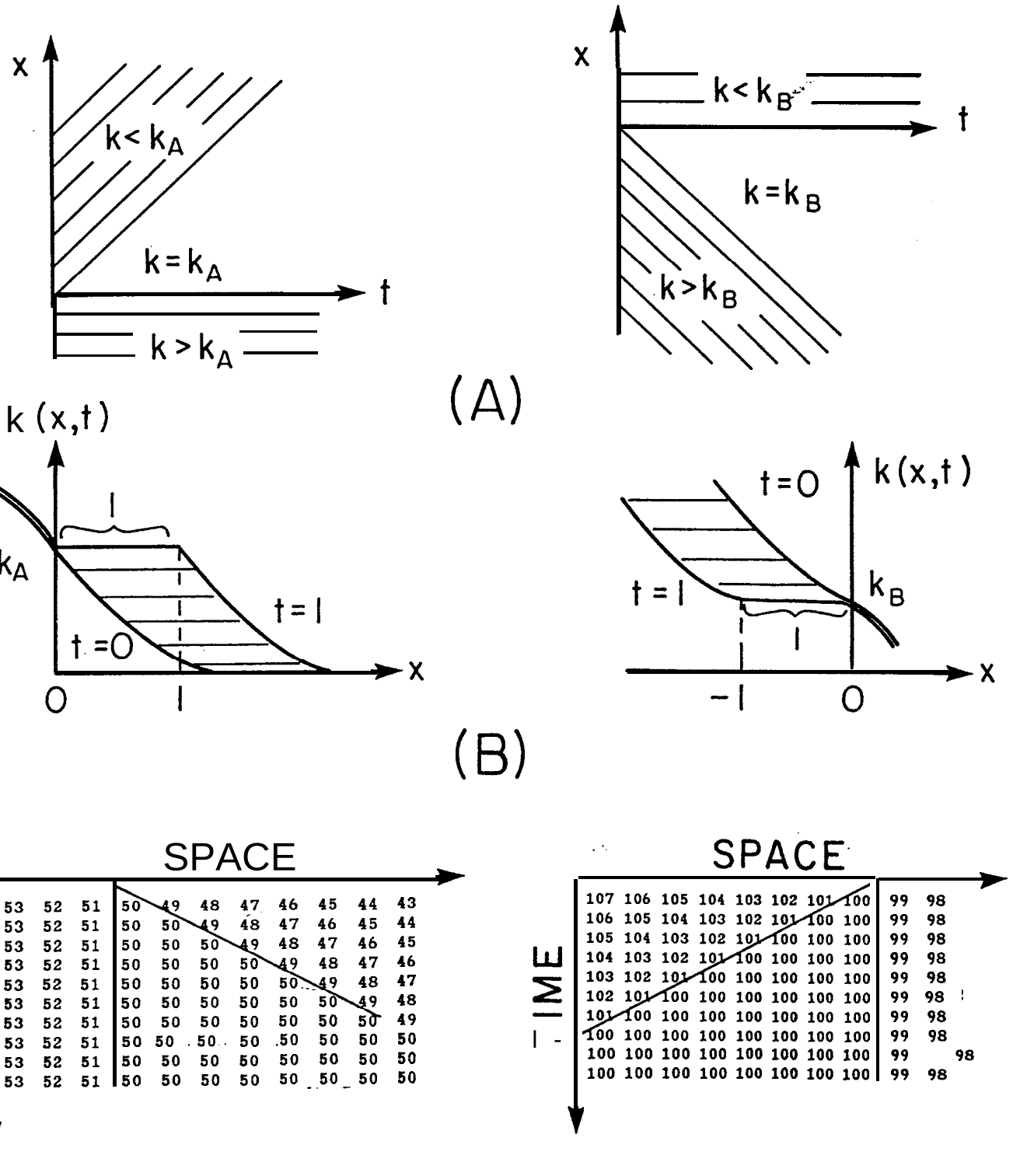

(c)

Figure 3. Traffic evolution with a decreasing density. (a) Map of characteristics. (b) Density profile. (c) Numerical result.

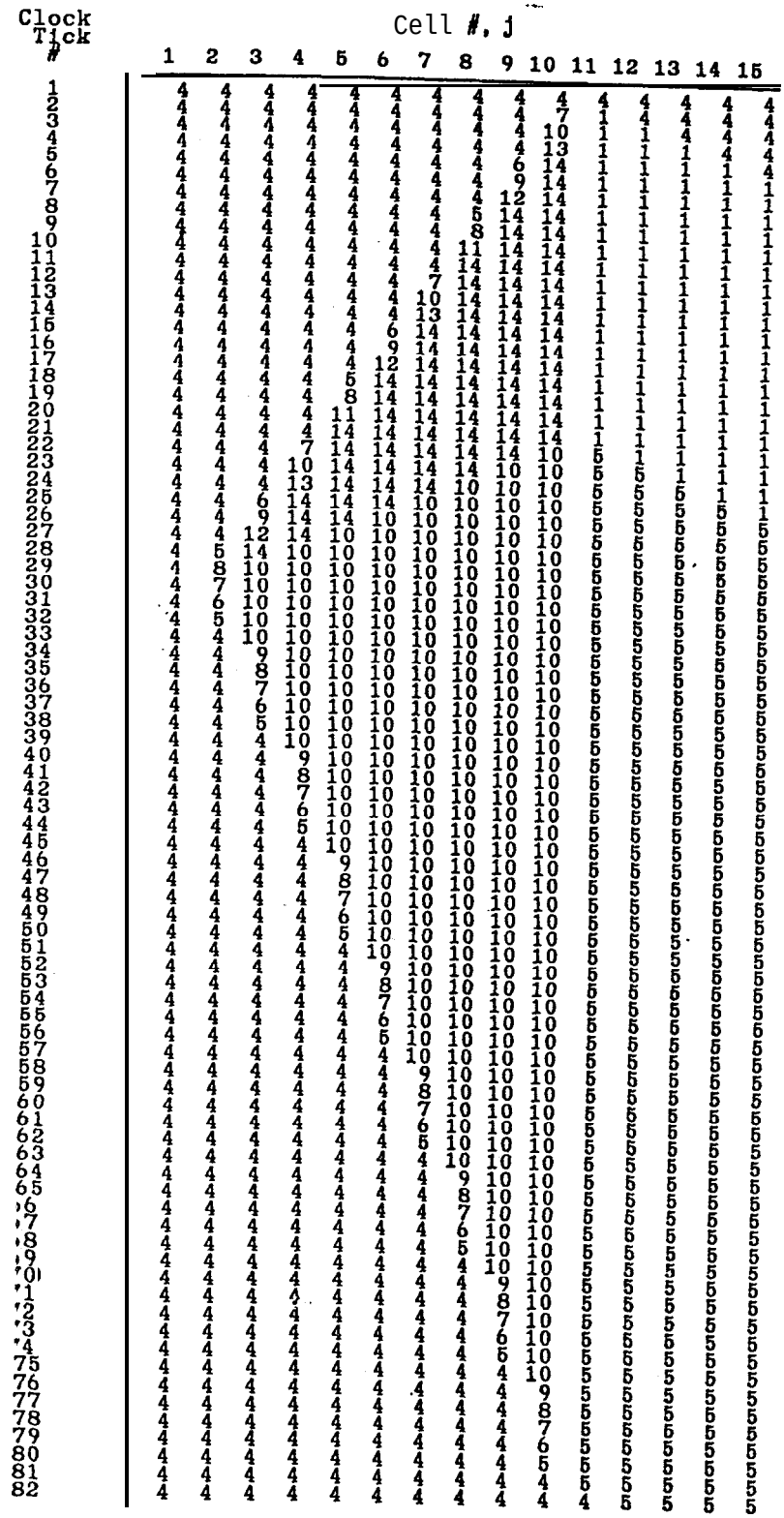

Figure 4. Numerical result for an example. The exhibit displays the contents of all cells as a function of time.

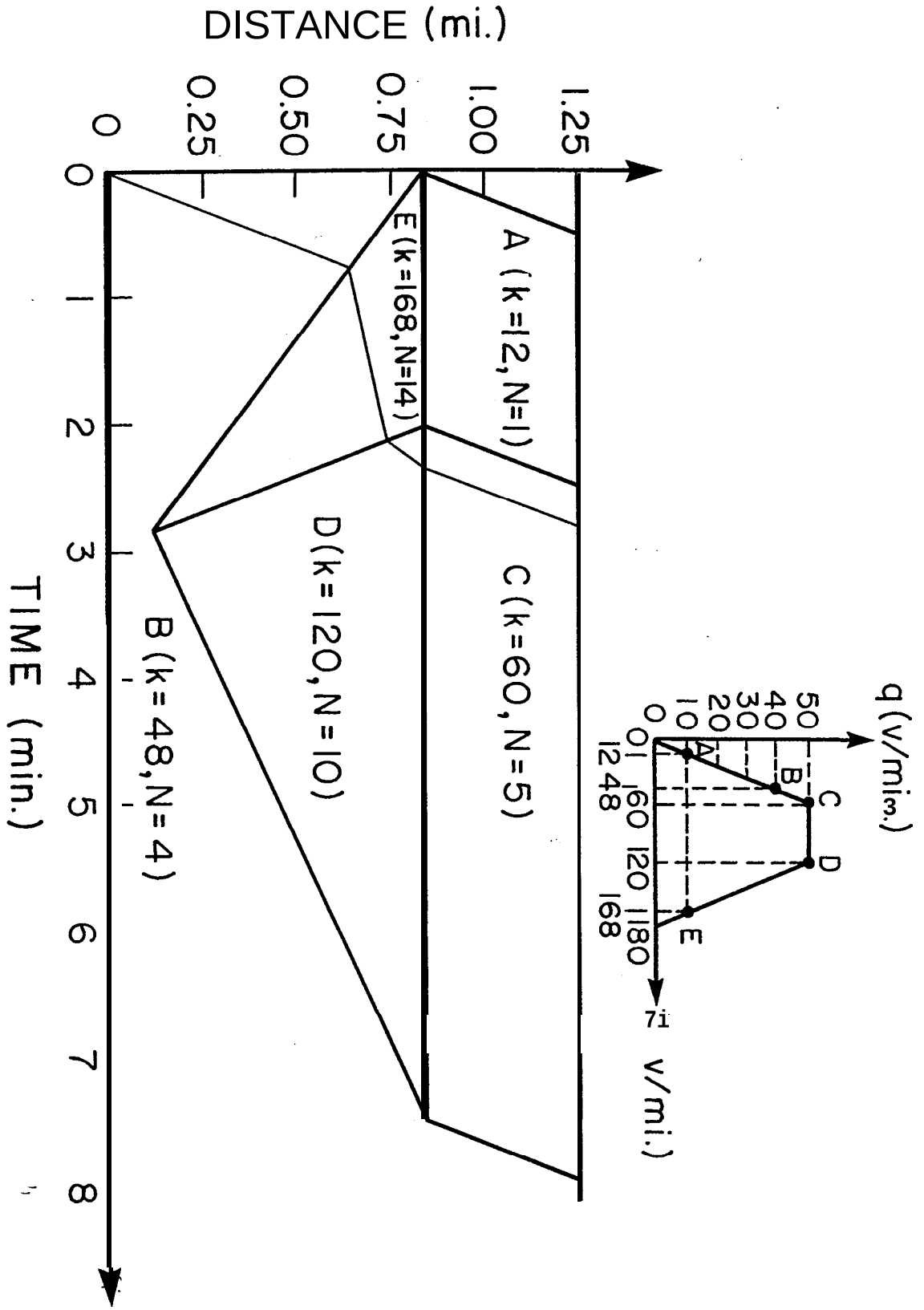

Figure 5. Hydrodynamic theory result for the same example.

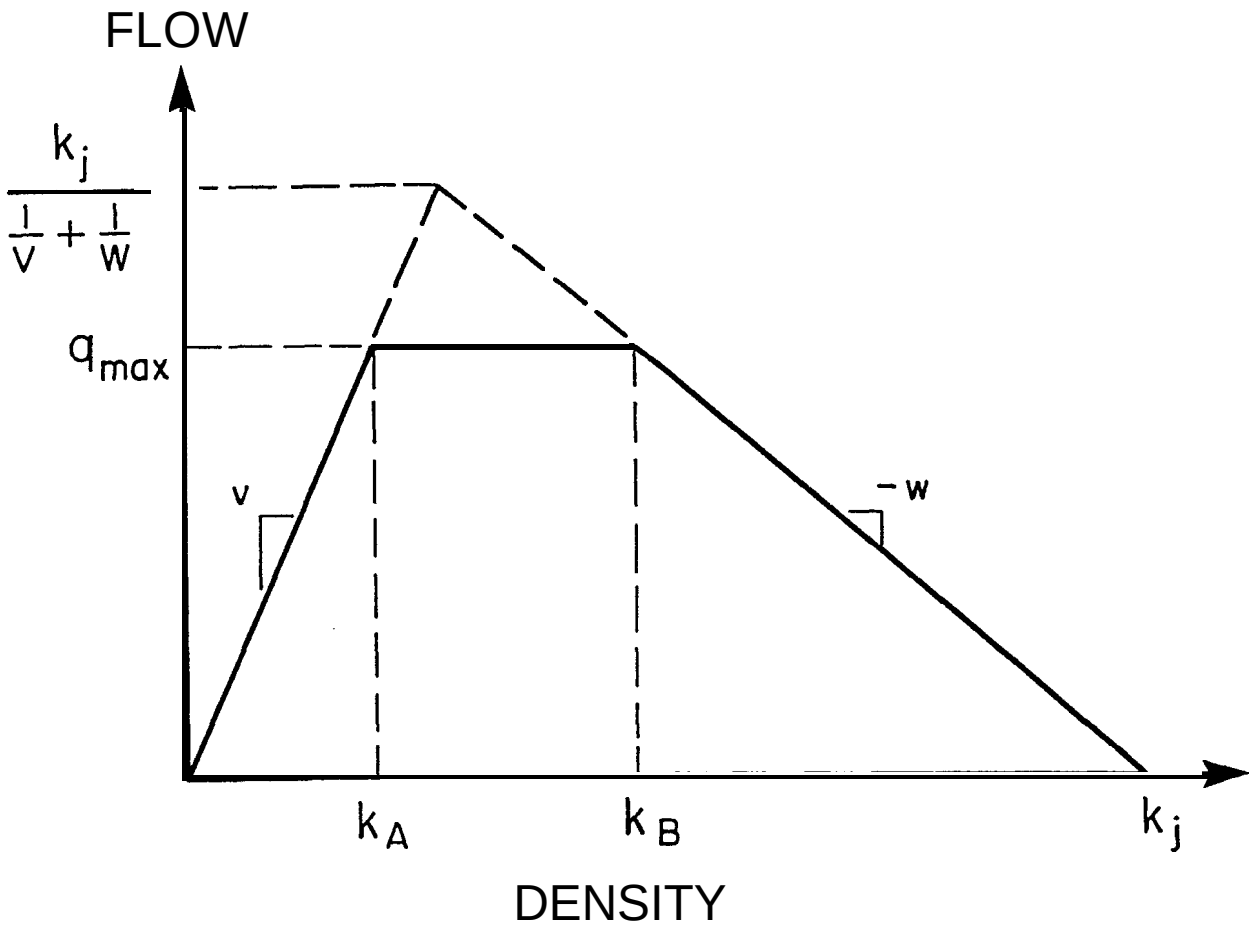

Figure 6. Flow-density relationship for the generalized cell-transmission model.

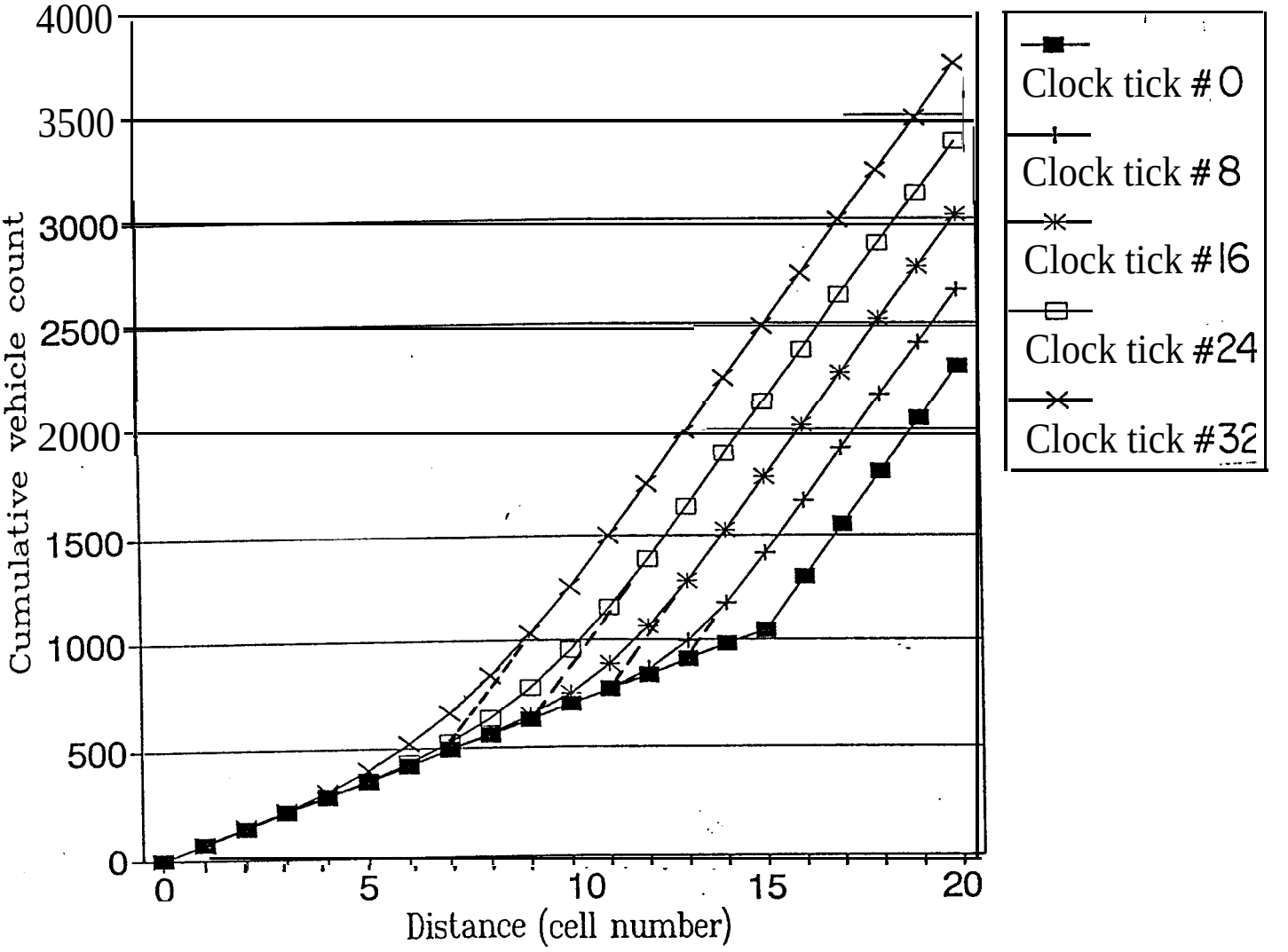

Figure 7. Generalized cell-transmission model: softening of a shock with distance.

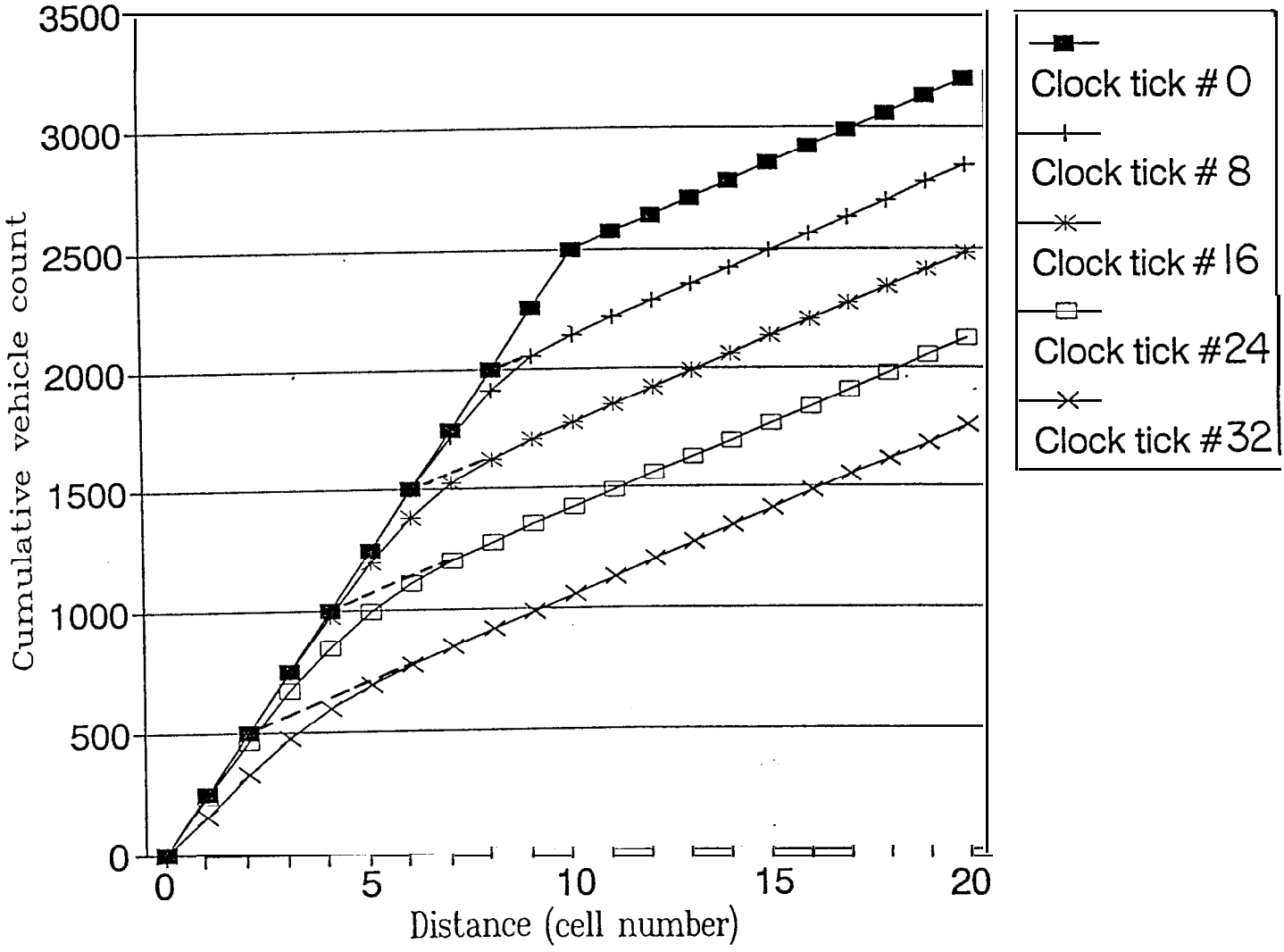

Figure 8. Generalized cell-transmission model: softening of an acceleration wave with distance.

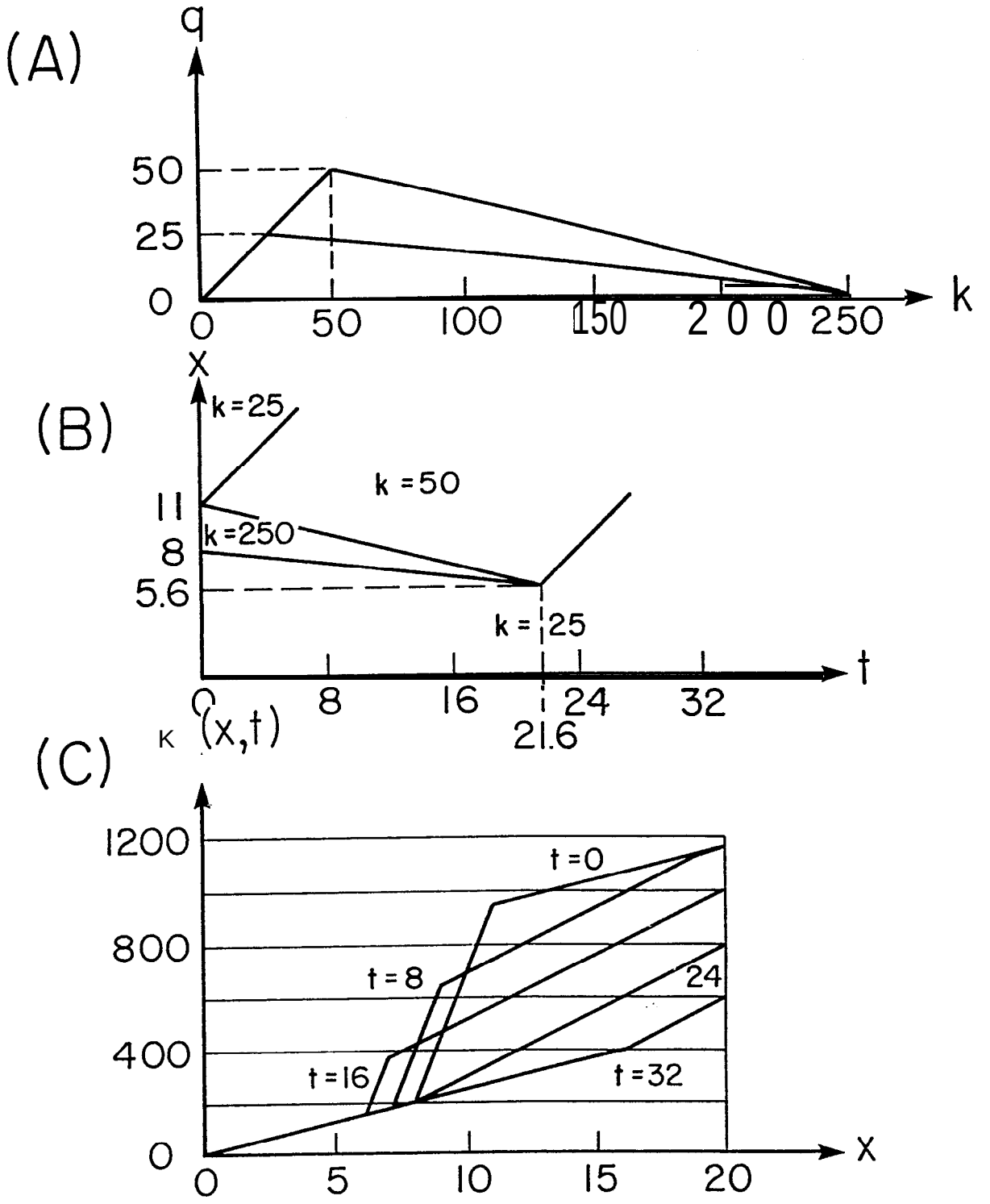

Figure 9. Hydrodynamic solution to an example with a generalized flow-density relationship. (a) The q-k relationship. (b) The resulting density map, k(x,t). (c) Cumulative density profiles at different times.

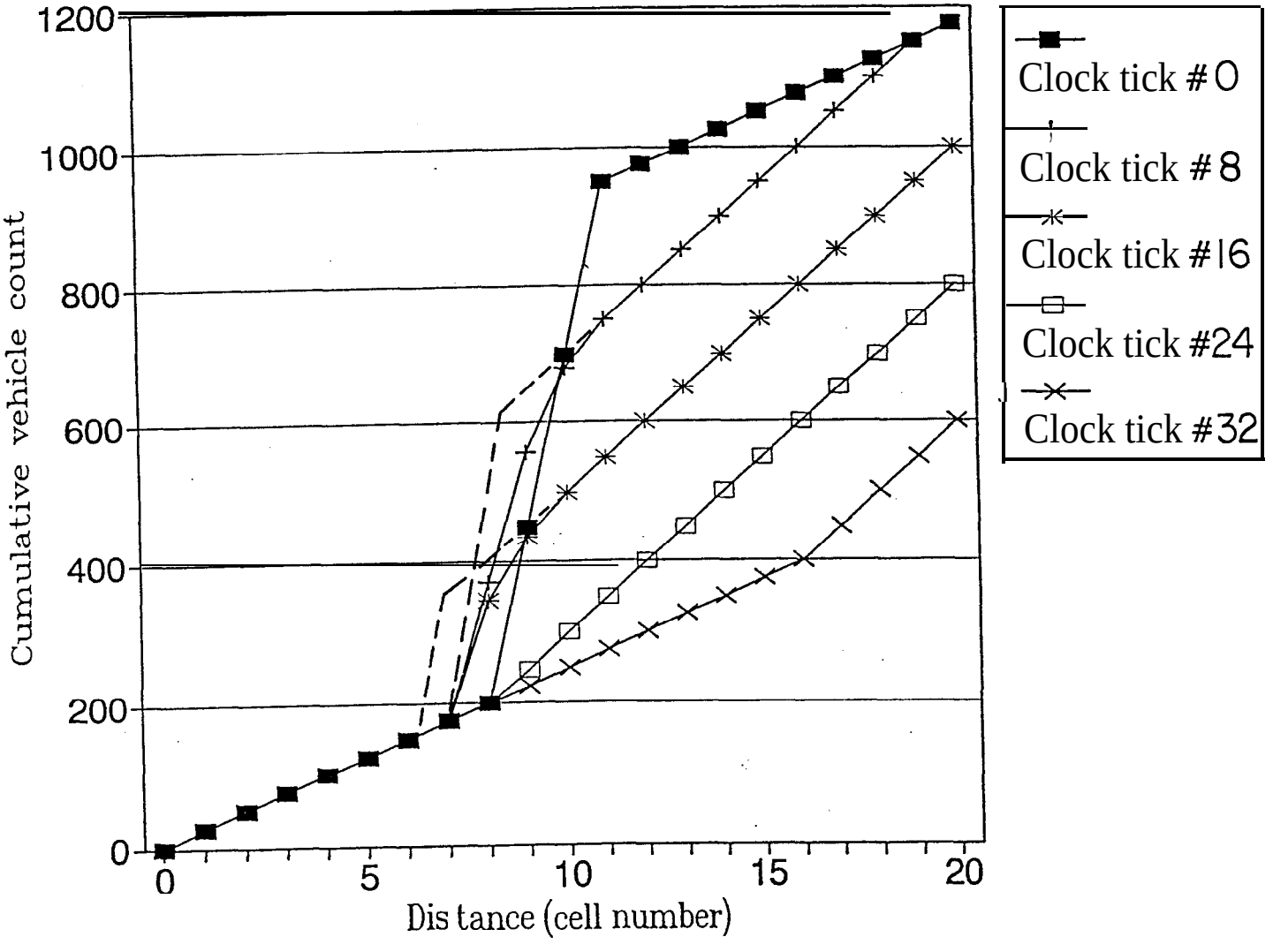

Figure 10. Cumulative density profiles predicted by the generalized cell-transmission model for the example of Fig. 9.

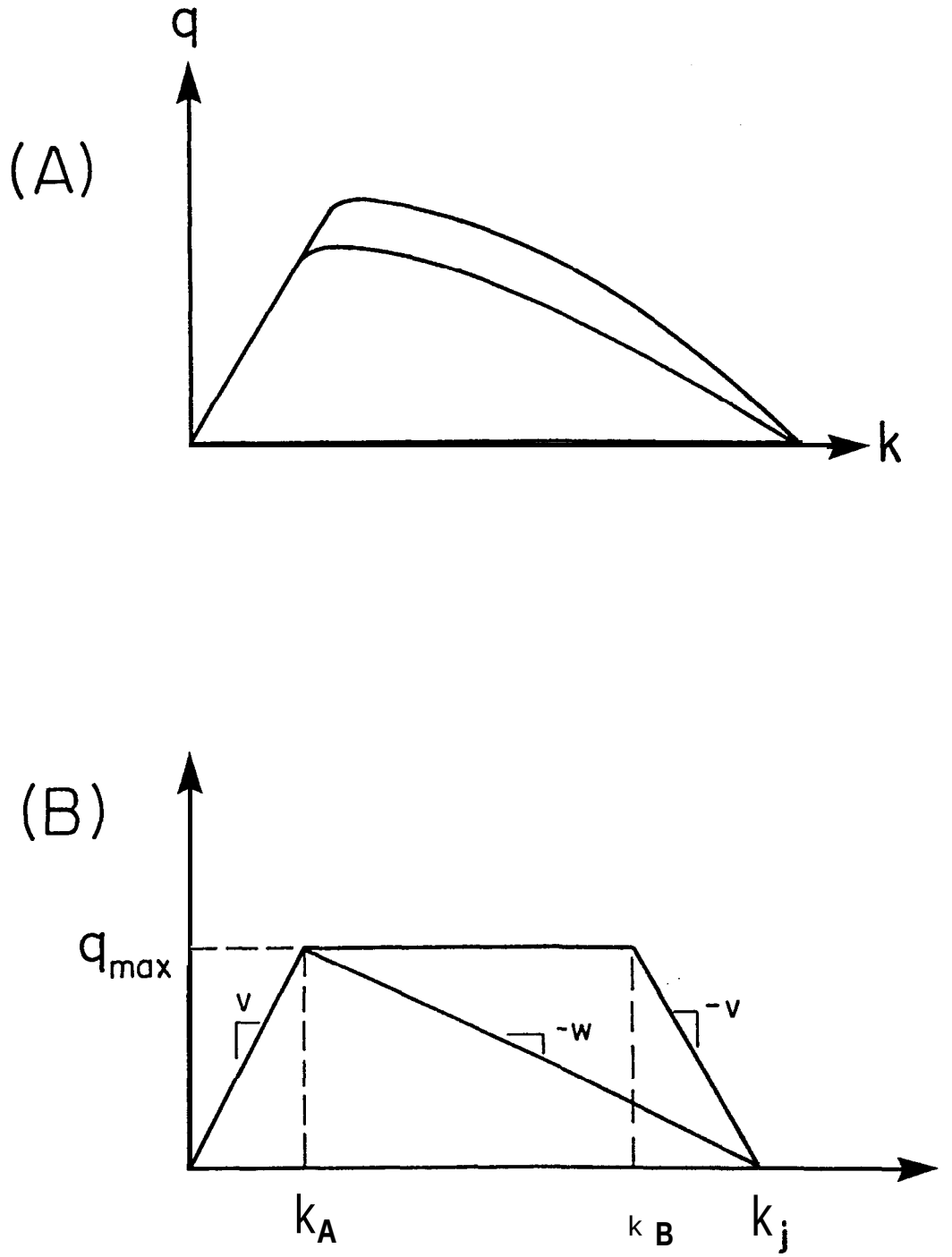

Figure 11. Flow-density relationships for the generalized cell-transmission model with built-in instability. (a) General case. (b) Specific case.

(A)

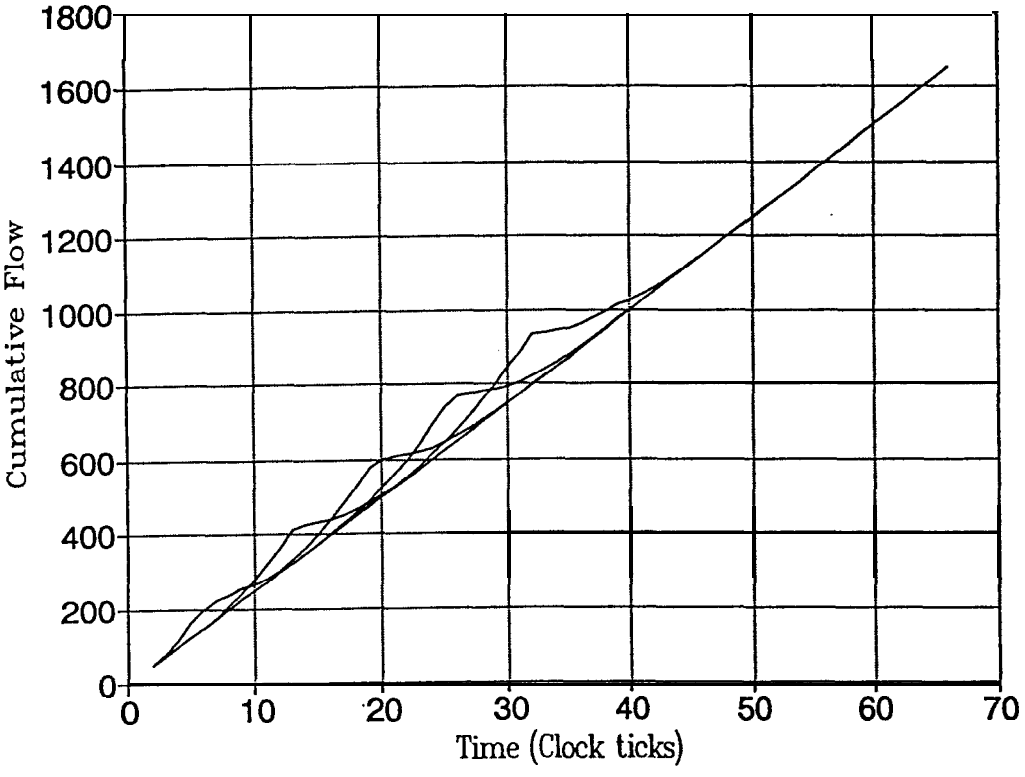

(B)

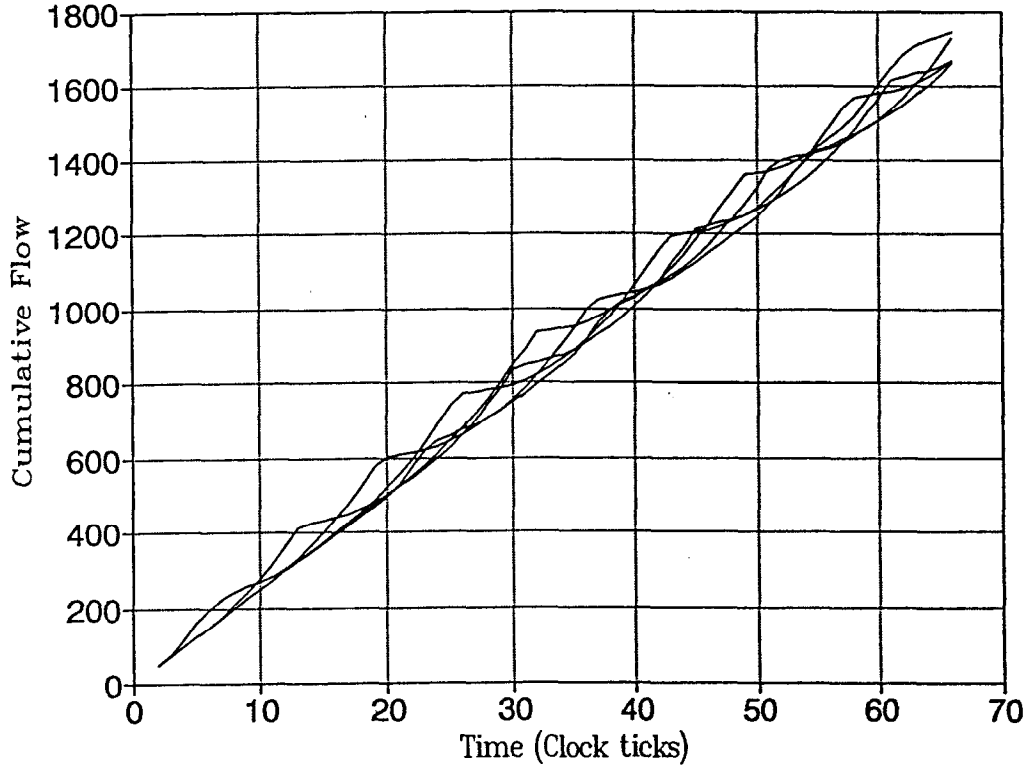

Figure 12. Curves of cumulative flow versus time observed at different positions. (a) A single impulse at the exit. (b) Steady noise at the exit.

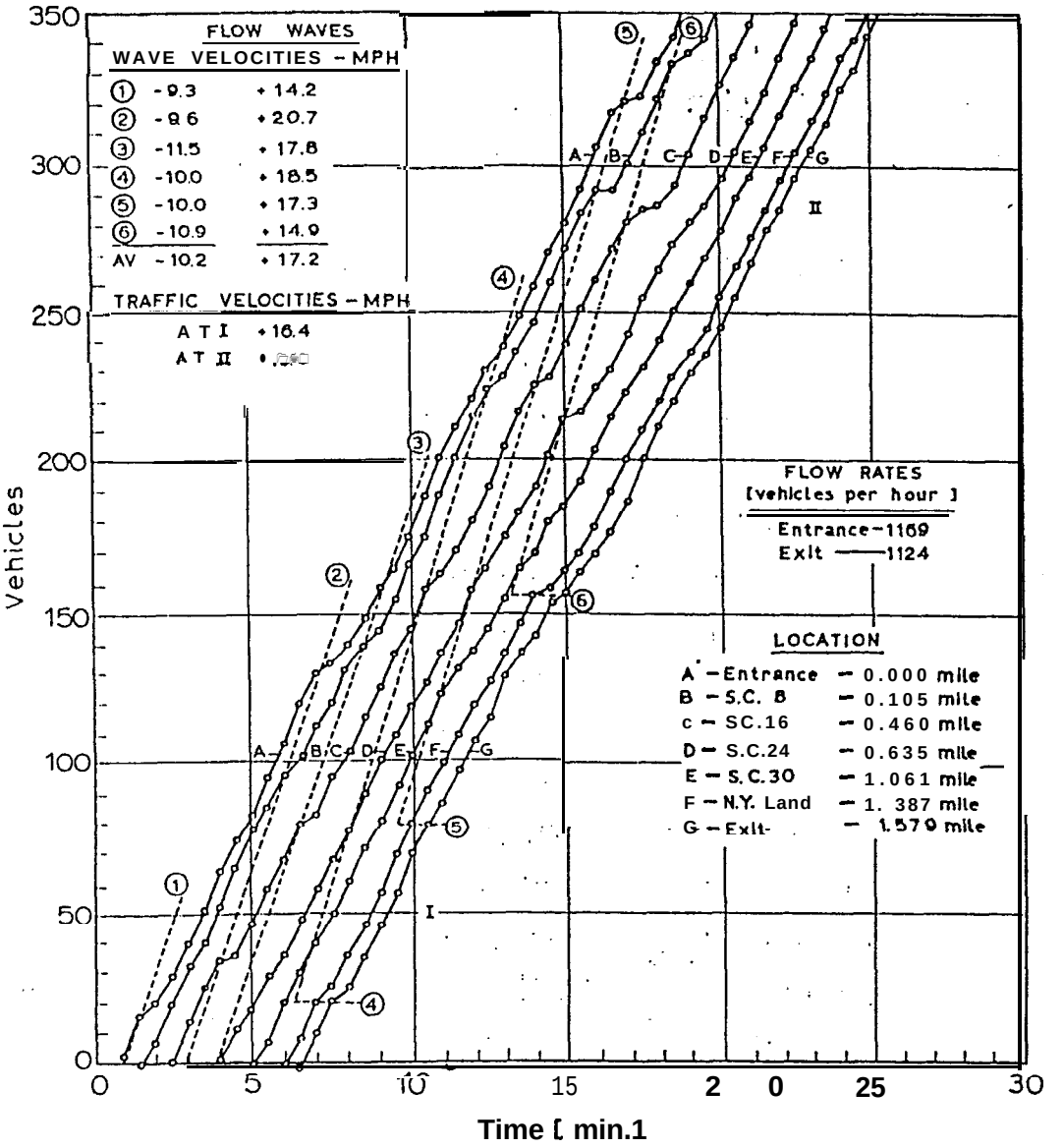

Holland tunnel, south tube, fast lane. Flow wave experiments.

Figure 13. Empirical cumulative curves of flow versus time, Edie and Foote **(1959).**

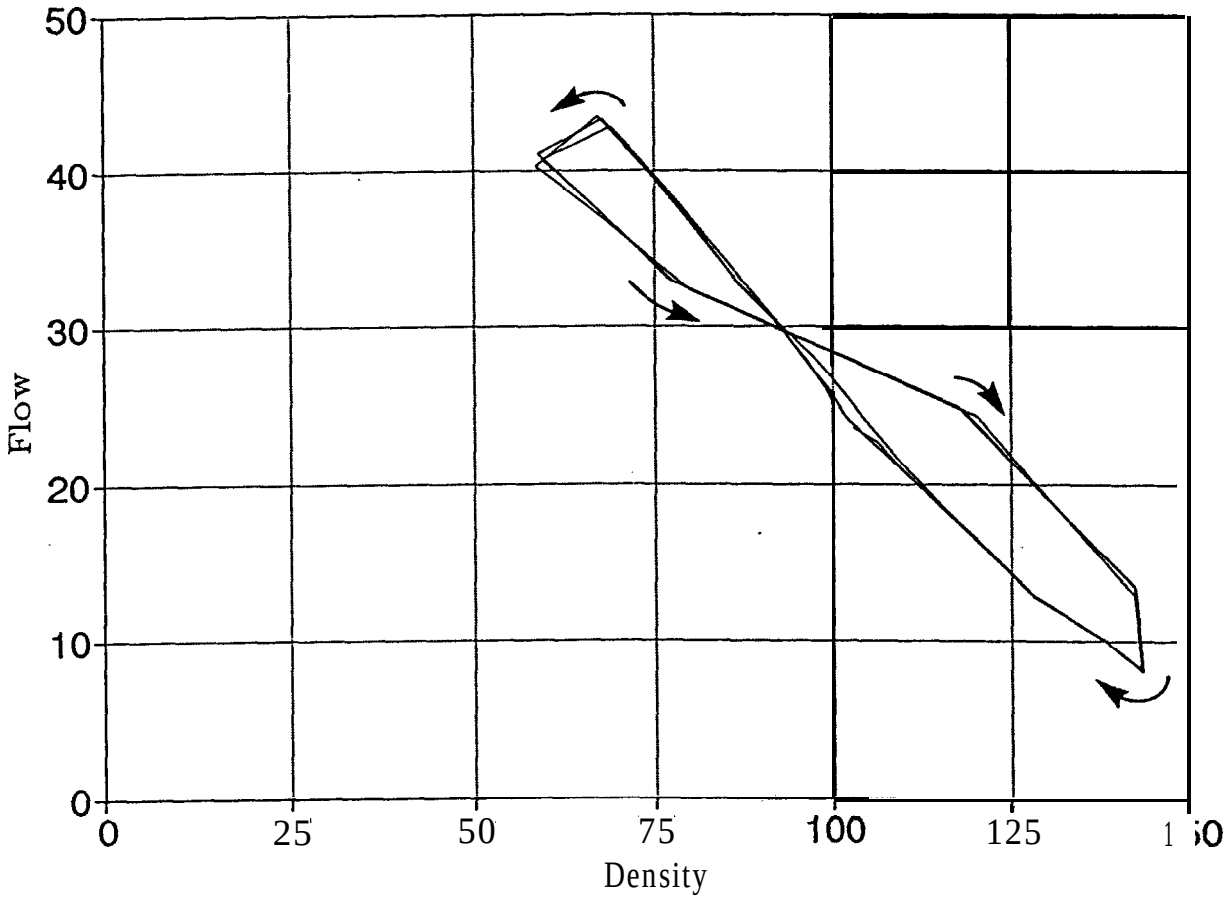

Figure 14. Flow-density hysteresis curve seen by a stationary observer.

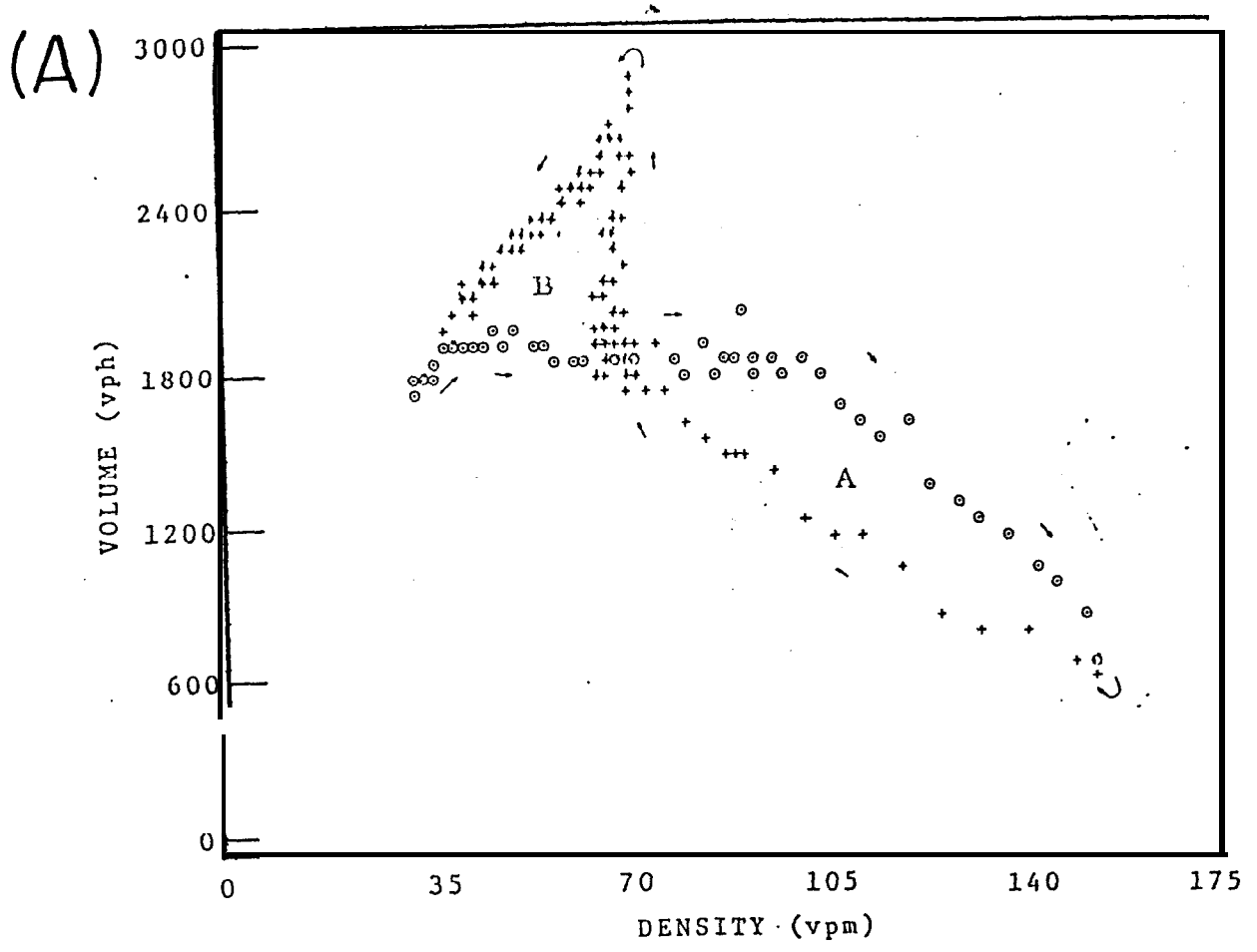

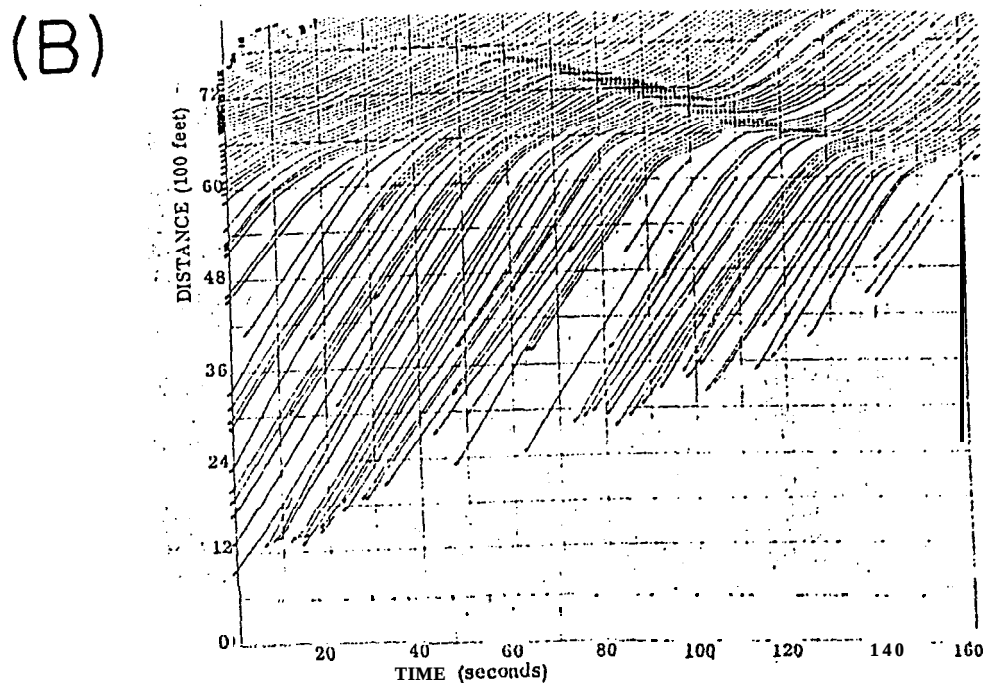

Figure 15. Empirical observations of Treiterer and Myers (1974). (a) Flow-density hysteresis. (b) Vehicle trajectories.